

Delayed nuclear fission

V. I. Kuznetsov and N. K. Skobelev
Joint Institute for Nuclear Research, Dubna

Fiz. Élem. Chastits At. Yadra **30**, 1514–1561 (November–December 1999)

The experimental techniques and results on delayed nuclear fission are reviewed. In this process the daughter nucleus produced in K capture of the parent nucleus undergoes fission from an excited state. The main experimental results are described. The qualitative theory of the process is discussed. The possibility of determining the fission barrier heights from the experimental data on delayed fission, in particular, on P_{DF} , the probability of delayed fission, is studied. Special attention is given to the techniques of measuring the main characteristics of the delayed-fission process. © 1999 American Institute of Physics. [S1063-7796(99)00406-4]

1. INTRODUCTION

Delayed fission is one of the fission modes of low-lying excited states, along with spontaneous fission and spontaneously fissioning shape isomers. Delayed fission gives additional information helpful for understanding the dynamics of the fission process as the excitation energy of the fissioning nucleus tends to zero.

Fission products with half-life on the order of minutes were first discovered in the Flerov Nuclear Reactions Laboratory in 1966 in experiments devoted to the synthesis of neutron-deficient heavy nuclei to seek spontaneously fissioning shape isomers.¹ The nuclei were then identified in reactions using beams of accelerated heavy ions, and it was concluded that they are the precursors of fissioning nuclides: their daughter nuclei are most likely to undergo fission from an excited state after K capture of the parent nucleus (see Fig. 1).^{2–4} This type of fission of neutron-deficient heavy nuclei far from the β -stability line was given the name “delayed fission” by us in 1967 by analogy with delayed nucleon emission. The authors of those studies^{1–4} were awarded a certificate for the discovery of delayed nuclear fission on 12 July 1971 (Ref. 5).

In moving away from the β -stability line (as the neutron deficit or excess grows), the β -decay energy Q_β of heavy nuclei becomes comparable to the fission barrier height of the daughter nuclei and can even exceed it. As a rule, after β decay the daughter nuclei are not only in the ground state, but also in excited states. When the energy E^* of an excited state ($E^* \sim Q_\beta$) becomes comparable to or larger than the height B_f of the fission barrier of the daughter nucleus, the population probability in the region of B_f can become sizable, and fission will compete with other fast decay modes of the daughter nucleus, for example, γ or delayed-neutron emission. In addition, it is necessary that the probabilities of β^- decay or electron capture (EC) of the parent nucleus not be suppressed by decay processes occurring in parallel, for example, α decay in the region of neutron-deficient nuclei. If these conditions are satisfied, the fission of the daughter nuclei after EC or β^- decay can be observed experimentally. The half-life, measured from the time distribution of the fission fragments, is equal to the half-life of β decay of the

parent nucleus, because the fission of the daughter nucleus occurs over a time 10^{-9} – 10^{-17} sec.

1.1. The qualitative theory of delayed fission

Let us discuss some of the main characteristics of delayed fission. The most important one is the delayed-fission probability P_{DF} . It is equal to the ratio N_{if}/N_i , where N_i is the total number of EC or β^- decays of the parent nucleus and N_{if} is the number of decays accompanied by delayed fission.

One of the approximations frequently used for theoretical calculations is given by^{6,7}

$$P_{DF} = \frac{\int_0^{Q_i} W_i(Q_i - E) \frac{\Gamma_f}{\Gamma_{tot}}(E) dE}{\int_0^{Q_i} W_i(Q_i - E) dE}. \quad (1)$$

Here $W_i(Q_i - E)$ is the transition-probability function ($i = \text{EC for } K \text{ capture and } i = \beta \text{ for } \beta \text{ decay of the parent nucleus}$), $\Gamma_f/\Gamma_{tot}(E)$ is the ratio of the fission width of excited levels of the daughter nucleus to the total decay width of these states, E is the excitation energy of the daughter nucleus, and Q_i is either Q_{EC} or Q_{β^\pm} . At low excitation energies it is assumed that fission and γ emission are the main deexcitation channels.

It is usually assumed that other possible decay channels are not important and that $\Gamma_f/\Gamma_{tot}(E) = [\Gamma_f/(\Gamma_f + \Gamma_\gamma)](E)$, where Γ_f and Γ_γ are the fission and radiation widths, respectively. In β^- -delayed fission it is sometimes necessary to take into account the possibility of neutron emission.

The probability function $W_i(E)$ for a transition to a level E can be represented as a product of the Fermi function $f(Q_i - E, Z)$ and the strength function of β decay, $S_\beta(E)$:

$$W_i(Q_i - E) \approx f(Q_i - E, Z) S_\beta(E). \quad (2)$$

The Fermi function $f(Q_i - E, Z)$ reflects the kinematics of beta decay and can be written as $f = (Q_{EC} - E)^2$ in the case of K capture (writing the Fermi function in this form presupposes the absence of β^+ decay) and as $(Q_\beta - E)^5$ for β decay. The strength function $S_\beta(E)$ is the distribution in excitation energy of the squared matrix elements of the β -decay type—the Fermi, Teller, etc., matrix elements. At

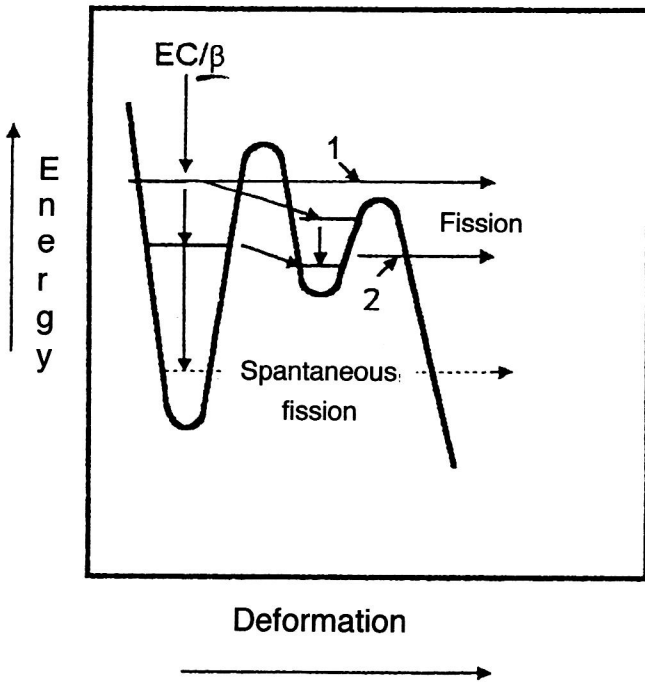


FIG. 1. Decay scheme of a nucleus undergoing delayed fission.

low excitation energies below the β -decay energy Q_β the strength function determines the nature of the decay and the half-life of the nucleus.

The question of the strength function of β transitions is not completely resolved. Various models are used to calculate $S_\beta(E)$. In the statistical model, (i) S_β is assumed to be constant above a given cutoff energy C in qualitative calculations, i.e., $S_\beta(E) = \text{const}$ for $E > C$ and $S_\beta(E) = 0$ for $E < C$; (ii) it is assumed that $S_\beta(E) \sim \rho(E)$, where $\rho(E)$ is the level density of the daughter nucleus.

In resonance nonstatistical models $S_\beta(E)$ is calculated on the basis of the gross theory of β decay. In the nonstatistical approach the energy dependence of $S_\beta(E)$ determines the nuclear structure and the isovector parts of the effective nucleon–nucleon interaction.

If the β -decay probability contains the contribution of several levels, and if delayed fission occurs from a level of energy E^* , then

$$P_{\beta\text{DF}} = \frac{\Gamma_f(E^*) S_\beta(E^*) f(Z, Q_\beta - E^*)}{\Gamma_{\text{tot}}(E^*) \sum S_\beta(E_i) f(Z, Q_\beta - E_i)}. \quad (3)$$

Klapdor *et al.*⁸ have shown that the calculated characteristics of delayed fission are significantly affected by low-lying structures of the β -decay strength function.

The dependence of P_{DF} on the level-population energy and on the structure of the fission barrier arises mainly from the fission width entering into the expression $[\Gamma_f/(\Gamma_f + \Gamma_\gamma)](E)$. The quantities $\Gamma_f(E)$ and $\Gamma_\gamma(E)$ are the fission and radiation widths, respectively. The radiation width $\Gamma_\gamma(E)$ is estimated⁶ from the γ -transition probabilities P_γ :

$$\Gamma_\gamma = \frac{P_\gamma}{2\pi\rho} = \frac{C_\gamma \Theta^4 \exp(E/\Theta)}{2\pi\rho}, \quad (4)$$

where ρ is the nuclear-level density, C_γ is a constant equal to $9.7 \times 10^{-7} \text{ MeV}^{-4}$, and Θ is the nuclear temperature (0.5–0.6 MeV).

The fission width $\Gamma_f(E) = P_f(E)/2\pi\rho$ also obviously depends on the fission-barrier penetrability P_f . The barrier penetrability of heavy nuclei is calculated on the basis of the simplified expression $P_f \approx P_A(E) \times R_B$, where $P_A(E)$ is the penetrability of the inner barrier and R_B is the transmission coefficient determining the fission of the nucleus from the lowest state of the second potential well. This assumption requires that fission does not occur until the nucleus is in the lowest level of the second potential well. In this case the calculation of $P_f(E)$ becomes much simpler. The passage through the inner barrier B_A reduces to the problem of tunneling through a parabolic barrier according to the formalism of Hill and Wheeler:⁹

$$P_A = \left\{ 1 + \exp \left[\frac{2\pi(B_f - E)}{\hbar\omega_f} \right] \right\}^{-1}, \quad (5)$$

where B_f is the barrier height and $\hbar\omega_f$ is the energy determining its curvature. Therefore, the fission width can be written as

$$\Gamma_f = \frac{R_B}{2\pi\rho} \left\{ 1 + \exp \left[\frac{2\pi(B_f - E)}{\hbar\omega_f} \right] \right\}^{-1} \quad (6)$$

and

$$\frac{\Gamma_f}{\Gamma_f + \Gamma_\gamma}(E) \approx \frac{R_B \left\{ 1 + \exp \left[\frac{2\pi(B_f - E)}{\hbar\omega_f} \right] \right\}^{-1}}{C_\gamma \Theta^4 \exp(E/\Theta) + R_B \left\{ 1 + \exp \left[\frac{2\pi(B_f - E)}{\hbar\omega_f} \right] \right\}^{-1}}. \quad (7)$$

Analysis of this expression shows that the term $\Gamma_f/(\Gamma_f + \Gamma_\gamma)$ depends strongly on the decay energy and on the structure of the fission barrier. With these assumptions, we can write down a simple equation for P_{EDF} , the probability of delayed fission after EC (ECDF):

$$P_{\text{EDF}} = \frac{\int_C^{Q_{\text{EC}}} (Q_{\text{EC}} - E)^2 \frac{\Gamma_f}{\Gamma_f + \Gamma_\gamma}(E) dE}{\int_C^{Q_{\text{EC}}} (Q_{\text{EC}} - E)^2 dE}. \quad (8)$$

Here C is the cutoff energy below which the strength function S_β is assumed equal to zero. In Ref. 10, C was determined from the dependence $C = 26A^{-1/2} \text{ MeV}$. The integral in the denominator of (8) is

$$\int_C^{Q_{\text{EC}}} (Q_{\text{EC}} - C)^2 dE = \frac{1}{3} (Q_{\text{EC}} - C)^3 = 1/3 (Q_{\text{EC}} - 26A^{-1/2})^3 \equiv [N_{\text{EC}}(A)]^{-1}, \quad (9)$$

where $N_{\text{EC}}(A)$ is a normalization function. Then Eq. (8) takes the form

$$P_{\text{ECF}} = N_{\text{EC}}(A) \int_C^{Q_{\text{EC}}} (Q_{\text{EC}} - E)^2 \frac{\Gamma_f}{\Gamma_f + \Gamma_\gamma} dE. \quad (10)$$

Meanwhile, in the case of β^- decay $[N_\beta(A)]^{-1} \equiv \frac{1}{6}(Q_\beta - 26A^{-1/2})^6$.

The probability of β -delayed fission (β DF) can be written qualitatively as

$$P_{\beta\text{DF}} \approx N_\beta(A) \int_C^{Q_\beta} (Q_\beta - E)^5 \frac{\Gamma_f}{\Gamma_\gamma + \Gamma_f}(E) dE. \quad (11)$$

In order to detect delayed fission in the region $Z > 89$, where the barrier heights lie in the range 4–6 MeV, it is necessary to study nuclei with Q_β of the same order of magnitude. In general, delayed fission after EC occurs with larger probability than after β^- decay. This follows from the form of the Fermi function for these decays. The Fermi function tends to zero in the case of β^- decay more rapidly than in EC. It would therefore be easier to study ECDF even if there were none of the well known difficulties of synthesizing neutron-rich nuclei. It should be noted that the given theoretical dependences can be used only for qualitative estimates.

The problems associated with the nature of the strength functions and their resonance structure in various regions of delayed fission (for nuclei with $Z > 89$, N near 126, or Z near 82) have been studied in extensive reviews.^{11,12}

A quantitative model must include a more detailed treatment of the passage through the fission barrier and eliminate the simplification associated with the assumption that the transition necessarily occurs to the lowest level in the second potential well.

The conditions allowing the experimental observation of delayed fission are readily satisfied in odd–odd neutron-deficient nuclei.

The large value of Q_β in comparison with that in neighboring nuclei, due to the odd–odd effect, means that Q_β and B_f are comparable even at a relatively short distance from the β -stability line. The competing α decay in parent nuclei with K capture is slowed down. The large neutron binding energy B_n in the even–even daughter nucleus allows the competition from the delayed-neutron channel to be neglected. The density of low-lying levels of the even–even daughter nuclei is low. The latter fact and the weaker energy dependence of the Fermi function in K capture favor the population of higher-lying levels. In addition, the fissility of the even–even daughter nucleus is higher than that of odd daughter nuclei.

In Fig. 1 we show the scheme for delayed fission with the two-hump barrier which is usual for heavy elements. Various transition possibilities are indicated. States in the first potential well of the daughter nucleus are populated initially. Direct population of the second potential well is forbidden because it would require a significant rearrangement of the nucleons of the nucleus simultaneously with β /EC decay. The nucleus can go from the first potential well to a state of energy E in the second well and divide. Return to the ground state of the daughter nucleus is very probable during these stages.

The probability for decay via the delayed-fission channel is very small, owing to competing processes. For example, the probability for delayed fission is $P_{\text{DF}} = N_{if}/N_i$, i.e., the ratio of the number of EC decays accompanying delayed

fission N_{if} to the total number of β /EC decays N_i is only ~ 0.01 in the most favorable cases of neutron-deficient nuclei. This suggests that the experimental study of such nuclei is quite difficult.

2. THE MAIN EXPERIMENTAL RESULTS

2.1. The discovery of the delayed fission of neutron-deficient nuclei

Delayed fission was first observed in the bombardment of a ^{233}U target by ^{10}B and ^{11}B ions accelerated at the U-300 cyclotron.¹ These experiments were specially designed to search for fissioning nuclei in the region of large neutron deficit. The experimental technique used at that time was therefore highly sensitive and allowed the detection of fissioning nuclei produced with an effective cross section of $(0.1\text{--}1.0) \times 10^{-35} \text{ cm}^2$ and half-lives of at least 1 sec. The observation of nuclei with such small cross sections was facilitated by bombarding the target by an internal heavy-ion beam at the U-300 cyclotron. The heavy-ion intensity attained was high ($\sim 100 \mu\text{A}$ for B^{+2} or Ne^{+4} ions), because the phase losses occurring in the outer orbits of a classical cyclotron and beam-extraction system were eliminated. The energy of the accelerated beam was easily controlled by moving the target along the radius of the magnetic pole of the cyclotron.

The bombardment was done on a sample with a slanted target allowing high currents to be obtained, and the fission fragments were recorded by means of movable, low-background, solid-state track detectors with efficiency 0.90 ± 0.05 . The slope of the target relative to the beam axis was 12° (Fig. 2). (The angle α between the axis of the accelerated-ion beam and the normal to the target plane was 78° .) Thus, the beam energy and the bombarded matter were distributed over an area 4.81 times larger than if the target were positioned perpendicular to the beam. It was thus possible to cool the target by simple methods. Another advantage of the slanted target was the deceleration of the recoil nuclei produced in nuclear reactions in a thin surface layer of the target material. Its thickness d is obviously $d = R \cos \alpha$, where R is the maximum range of the accelerated ions in the target material. As a result, the target material did not affect the fission-fragment yield. The target and the screen over it acted as a Faraday cup. The target and the cooling circuit were electrically insulated. These measures allowed reliable measurement of the ion current (see Fig. 2).

After bombardment of the target by a given ion flux, the cyclotron beam was switched off and an automatic system successively placed four solid-state detectors over the target during a time close to the lifetime of the studied isotope with respect to K capture. At the start of bombardment of the target, the detector assembly was shifted to a chamber sufficiently far from the target in order to shield the detectors from scattered particles and neutron background. The procedure was repeated periodically.

The time to move the detectors from the storage chamber to the target was of order 3–3.5 sec. A cassette system was used which allowed the detectors to be replaced in a short time; this was particularly important, given the high

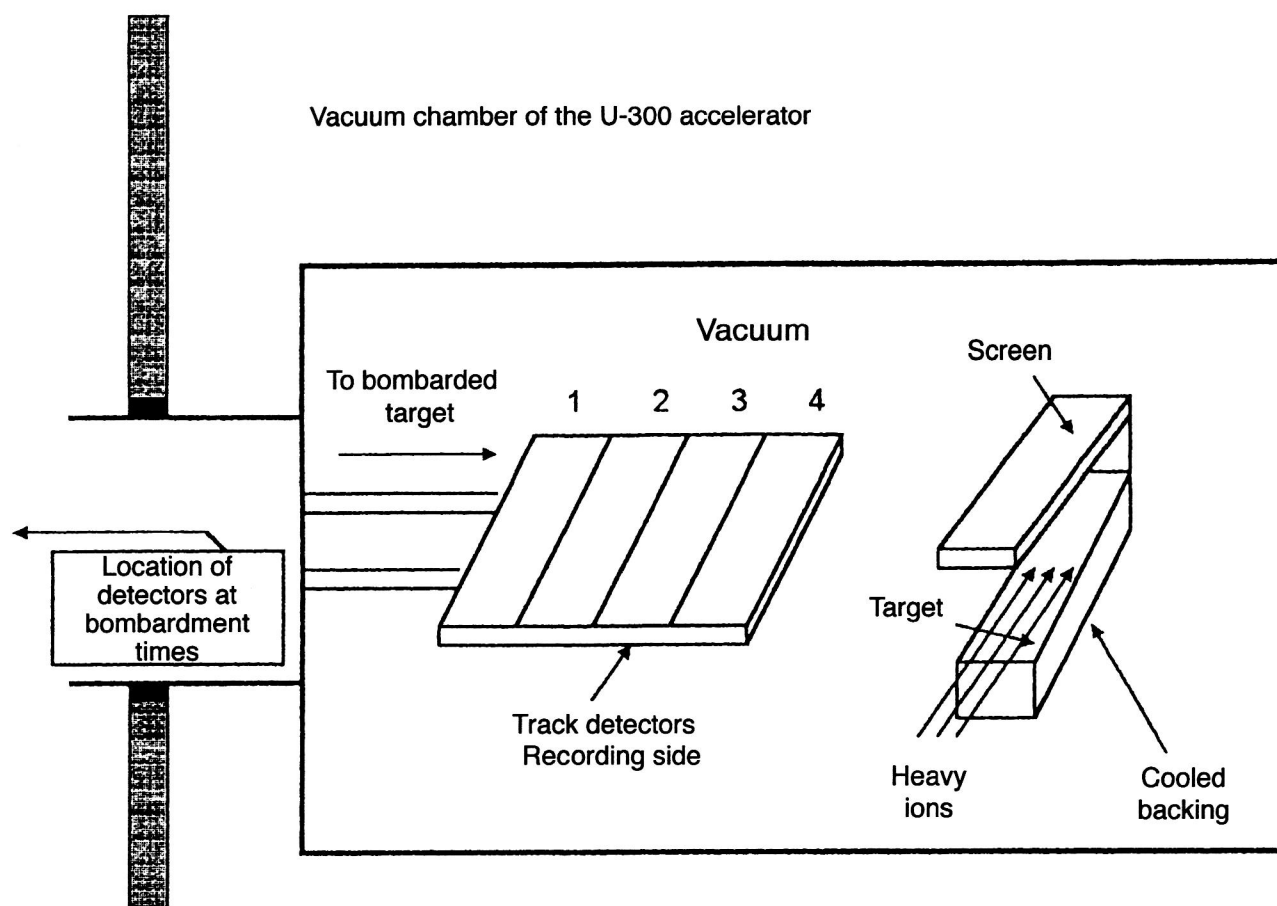


FIG. 2. Scheme for a sample with a slanted target. 1–4 are glass track detectors. The copper backing is cooled by water (the cooling system is not shown).

activation of the target in the experiments, when the intensity of accelerated heavy ions ensured the detection of fissioning nuclei with a production cross section of up to $\sim 1.0 \times 10^{-36} \text{ cm}^2$.

In the first experiments, the light uranium isotope ^{233}U was bombarded by ^{10}B and ^{11}B ions. The intensity of the accelerated boron ion beam reached 10^{14} particles/sec. At ^{11}B energy above 75 MeV the time distribution of the fragments corresponding to half-lives on the order of minutes was recorded. The decay curve of the synthesized nuclides was clearly split into two exponentials with half-lives $5 \pm 1 \text{ sec}$ and $2.6 \pm 0.2 \text{ min}$. Only the nuclear decay with $T_{1/2} = 2.6 \text{ min}$ was studied. The effect of the short-lived component was eliminated by keeping the detectors inside the chamber for 33 sec after the beam was switched off. The number of boron ions in each bombardment cycle was 6×10^{16} , and their range in the ^{233}U layer was 4.5 mg/cm^2 .

After the effect was discovered, the excitation function of the reaction leading to the production of fissioning nuclides with half-life $T_{1/2} = 2.6 \text{ min}$ was measured. A thin target was used for these measurements, so that the maximum energy losses of the ^{11}B ions in the bombarded material were less than 1 MeV. Along with measurement of the yield of fissioning nuclei, the decay curves were obtained for each energy of the accelerated ions (Fig. 3). The decay curves suggested that in the range of boron ion energy from 75 to 83 MeV, the same nuclide with $T_{1/2} = 2.6 \text{ min}$ was synthesized

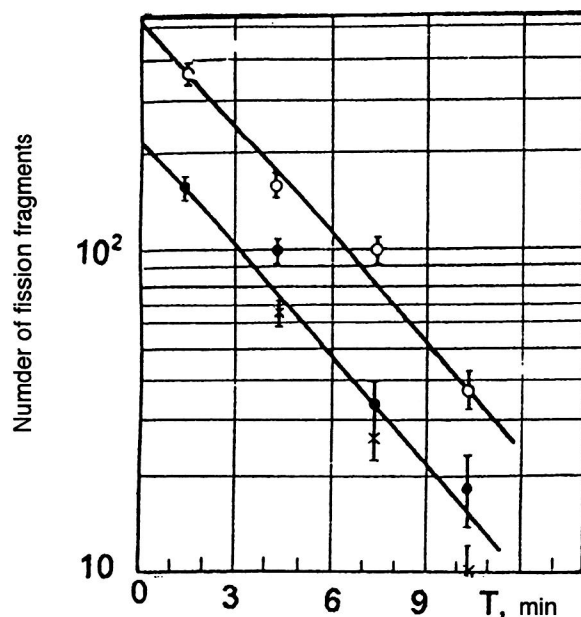


FIG. 3. Decay curves for $^{234}\text{Am} \rightarrow ^{234}\text{Pu} \rightarrow \text{ff}$ (fission fragments). The reactions $^{233}\text{U}(^{10}\text{B}, \alpha 5n)$ and $^{233}\text{U}(^{11}\text{B}, \alpha 6n)$. The light circles are for energy E of the ^{10}B ion equal to 60 MeV, the dark circles are for ^{11}B energy 75 MeV, and the crosses are for ^{11}B energy 80 MeV.

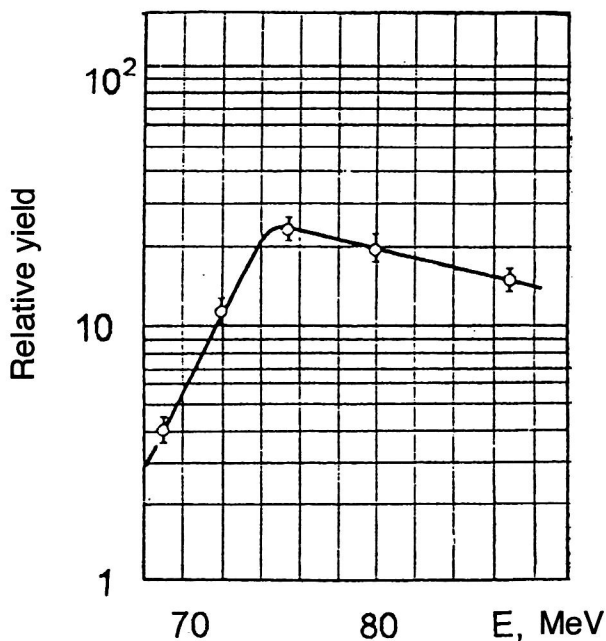


FIG. 4. Excitation function of the reaction $^{233}\text{U}(^{11}\text{B}, \alpha 6n)^{234}\text{Am}$.

in the reaction $^{233}\text{U} + ^{11}\text{B}$. The excitation function of the reaction is shown in Fig. 4. The calculation of the cross section for production of a fissile product in the energy range corresponding to the maximum yield gave $2.0 \times 10^{-33} \text{ cm}^2$. In the bombardment of ^{233}U by ^{10}B ions of energy 60 MeV, a fissioning product with roughly the same production cross section and half-life $T_{1/2} = 2.6 \text{ min}$ was also discovered. In control experiments, a thick ^{235}U target (4.5 g/cm^2) was bombarded by ^{11}B ions of energy 74 and 82 MeV and ^{10}B ions of energy 60 MeV. A ^{232}Th target was bombarded by ^{10}B ions of the same energy. No tracks from fragments of fissioning nuclei with half-lives on the order of minutes were recorded.

The control experiments confirmed the reliability of the data that had been obtained, and no background which could influence the experimental results was observed in them. However, the form of the excitation function for the reaction $^{233}\text{U} + ^{11}\text{B}$ did not correspond to that for evaporation reactions of the type $^{233}\text{U}(^{11}\text{B}, xn)$, whose excitation curve could be used to identify the synthesized nuclide. The excitation function was rather ill-defined, as in the case when a nucleus emits not only neutrons, but also charged particles.

The most probable explanation was that the observed fission fragments were the products of nuclei created in reactions like $^{233}\text{U}(^{11}\text{B}, \alpha xn)$ and $^{233}\text{U}(^{10}\text{B}, \alpha xn)$. It therefore appeared very likely that the evaporation reaction (HI, xn) with $x = 5$ or 6 in which nuclei with $T_{1/2} = 2.6 \text{ min}$ would be synthesized could occur on boron ions in the bombardment of a ^{230}Th target.

It is well known that it is difficult to obtain a pure ^{230}Th target, and therefore a mixture of oxides of the isotopes ^{230}Th and ^{232}Th was used. The hardness of the target was increased by adding organic compounds to the mixture, and the prepared mass was deposited in thin layers on an aluminum backing. The organic material was burned off after each

layer was deposited. The target thickness with respect to the ^{230}Th isotope was $250 \mu\text{g/cm}^2$. The range of the accelerated ions in the material was equivalent to that in pure ^{230}Th of thickness 1.2 mg/cm^2 . The maximum loss in the target material (taking into account the ^{232}Th isotope, the target thickness was 2.4 mg/cm^2) was $\sim 1.5 \text{ MeV}$.

In the bombardment of a target of "light" thorium by accelerated ^{10}B and ^{11}B ions in the energy range 50–90 MeV, fission fragments from nuclei decaying with a half-life of 2.6 min were recorded. The shape of the excitation function corresponded to evaporation reactions with emission of six and seven neutrons (for ^{10}B and ^{11}B , respectively) from the compound nucleus. The locations of the maxima of the excitation functions of the nuclear reactions $^{230}\text{Th}(^{10}\text{B}, 6n)^{234}\text{Am}$ and $^{230}\text{Th}(^{11}\text{B}, 7n)^{234}\text{Am}$ were found experimentally. At boron ion energies 70.5 MeV (^{10}B) and 82.0 MeV (^{11}B) the maxima coincided with the calculated values when the temperature T of the compound nucleus was computed on the basis of the systematics $T = f(A)$ (Ref. 13). For compound nuclei in the above reactions, $T = 1.5 \text{ MeV}$.

On this basis, the fissioning nuclei with half-life 2.6 min were identified as decay products of the americium isotope with mass number 234.

The presence of ^{232}Th in the target material did not affect the yield of the fissioning product with $T_{1/2} = 2.6 \text{ min}$, as was shown by control experiments in which a ^{232}Th target of thickness 5 mg/cm^2 was bombarded by boron ions of energy 70.5 MeV and 82.0 MeV. Here no fissioning products with half-life in the minute range were observed. The only possible background was that due to the fission of the traces of uranium contained in the glass solid-state detectors. The error that this introduced into the measurements was less than 5%.

The cross sections for production of ^{234}Am nuclei accompanied by fission in the reactions $^{230}\text{Th}(^{10}\text{B}, 6n)^{234}\text{Am}$ and $^{230}\text{Th}(^{11}\text{B}, 7n)^{234}\text{Am}$, calculated on the basis of the experimental data, were $(5.7 \pm 0.5) \times 10^{-34} \text{ cm}^2$ and $(5.4 \pm 0.5) \times 10^{-34} \text{ cm}^2$, respectively, at the maxima of the excitation functions. In that study, published in 1967 (see Ref. 3), the authors concluded that "the possibility of delayed fission cannot be excluded if the ^{234}Pu nucleus with high excitation energy is produced in the K capture of ^{234}Am ."

When the energy of the accelerated ^{10}B ions exceeded 82 MeV, fissioning nuclei with half-life 1.40 min were observed. The maximum of the excitation function of this emitter was shifted by 12 MeV to higher energies relative to the maximum of the excitation function of $^{230}\text{Th}(^{10}\text{B}, 6n)$. The effect of the decay of this isotope was taken into account in calculating the cross section for production of the fissioning product in the synthesis of ^{234}Am .

The discovered fission of nuclei with half-life $T_{1/2} = 1.40 \text{ min}$ was studied in specially designed experiments. The target bombardment time, the delay before the start of recording fission fragments, and the time during which the detector was located above the target were chosen so as to optimize the detection of the fission fragments of the product with half-life 1.40 min. The total efficiency of recording fission fragments was about 15% (taking into account the loss to decay during the bombardment and delay

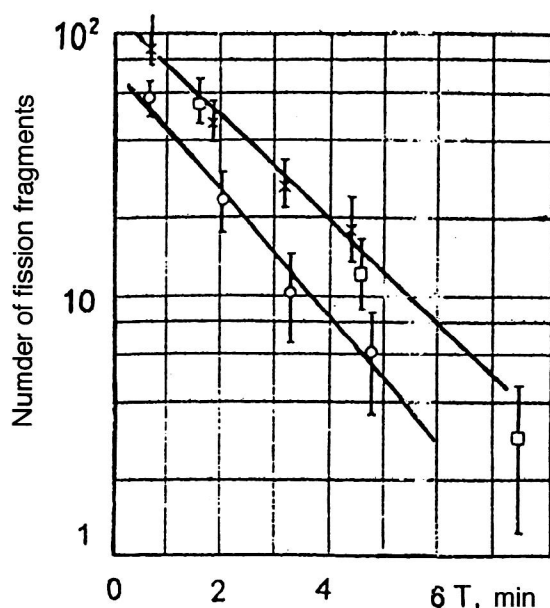


FIG. 5. Decay curves of the isotope ^{232}Am , obtained by recording fragments of delayed fission from the reaction $^{230}\text{Th}(^{10}\text{B}, 8n)^{232}\text{Am}$ at various energies of the ^{10}B ions. The crosses and light squares are for energy 88.5 MeV, and the light circles for 82.0 MeV.

times). The decay curves are shown in Fig. 5. In Fig. 6 we show the excitation function of the fissioning nuclide with half-life 1.40 min for normalization of the number of fragments at each point to 2.53×10^{17} ^{10}B ions. The excitation function has the bell shape typical of the (HI, xn) reaction. From the location of the maximum of the excitation function and its width at half-max, it followed that fission fragments from the product of the reaction $^{230}\text{Th}(^{10}\text{B}, 8n)^{232}\text{Am}$ had been observed. Therefore, the fissioning nuclide with half-life 1.40 min was identified as a product of the ^{232}Am iso-

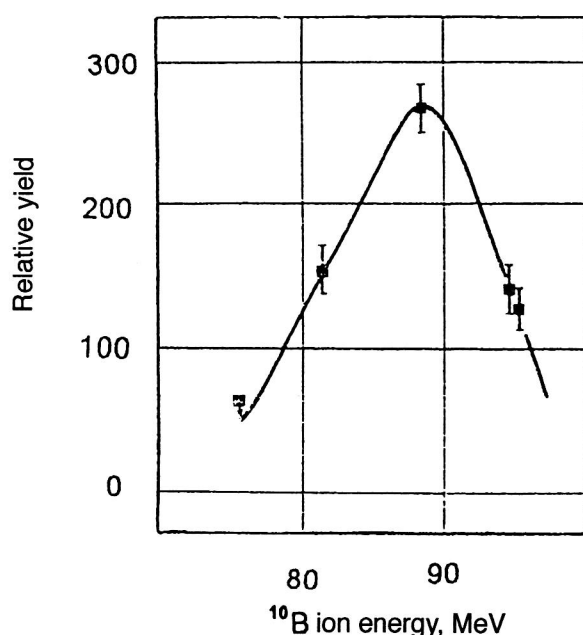


FIG. 6. Excitation function of the reaction $^{230}\text{Th}(^{10}\text{B}, 8n)^{232}\text{Am}$.

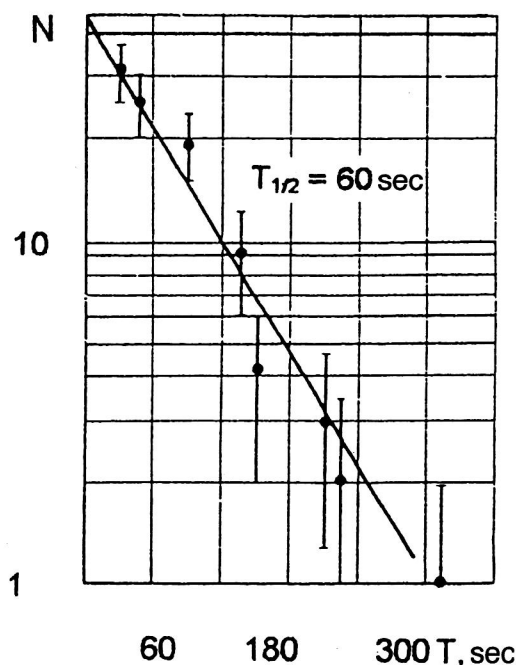


FIG. 7. Decay curve for fissioning products of the reaction $^{209}\text{Bi}(^{22}\text{Ne}, 3n)^{228}\text{Np}$.

tope. The cross section for ^{232}Am production measured at the maximum of the excitation function was $(2.3 \pm 0.4) \times 10^{-33} \text{ cm}^2$.

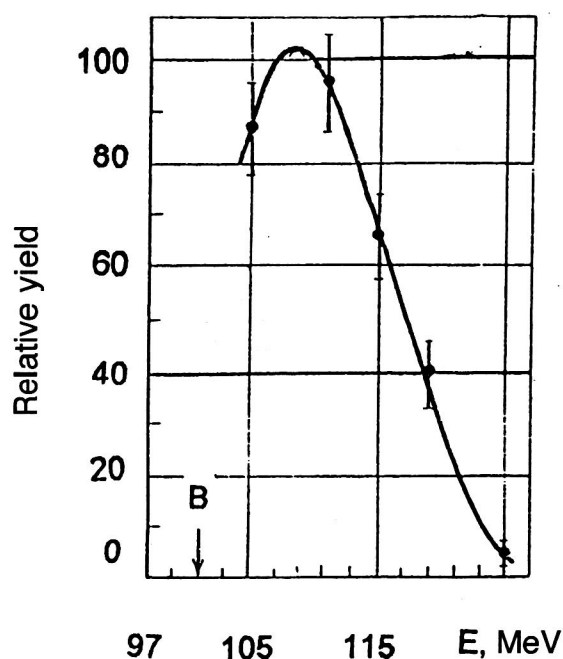
In their study published in 1967, the authors concluded:² “The ^{232}Am nucleus with half-life 1.40 min undergoes K capture, which is possible if it starts from the energy expected for electron capture. In decay to excited levels of the ^{232}Pu isotope close to the top of the fission barrier, fission from these states occurs.”

Analysis of the half-lives and decay energies of light isotopes of Np with respect to EC and α decay and extrapolation of their values to unknown neutron-deficient neptunium nuclei led to the conclusion that the delayed fission of Np isotopes could be observed.

To check this idea, a slanted bismuth target of effective thickness 9.5 mg/cm^2 was bombarded by accelerated ^{22}Ne ions with intensity 10^{14} particles/sec. The bombardments lasted 4 min, and then, after the cyclotron beam was switched off, solid-state detectors were placed above the bombarded matter successively at one-minute intervals. As a result, a fissioning isotope with half-life 60 ± 5 sec was found in the bombardment of a bismuth target by ^{22}Ne ions accelerated to 110 MeV (Ref. 4).

In Fig. 7 we show the decay curve obtained in two independent experiments. Solid-state track detectors were also used to record fission fragments. The excitation function of the fissioning product was obtained by bombarding a thin bismuth target by $^{22}\text{Ne}^{+4}$ ions. The ion range in the target was 2.10 mg/cm^2 . The background due to the fission of uranium impurities in the detectors was monitored according to the number of tracks on opposite sides of the detectors inaccessible to fission fragments from the nuclear reaction $^{209}\text{Bi}(^{22}\text{Ne}, xn)$.

The shape and location of the maximum of the excitation

FIG. 8. Excitation function of the reaction $^{209}\text{Bi}(^{22}\text{Ne}, 3n)^{228}\text{Np}$.

function of the nuclide with half-life $T_{1/2} = 60$ sec (Fig. 8) corresponded to a nuclear reaction occurring via the formation of a compound nucleus followed by evaporation of three neutrons.

The synthesis of fissioning isotopes in the reactions $^{209}\text{Bi}(^{22}\text{Ne}, p2n)$ and $^{209}\text{Bi}(^{22}\text{Ne}, \alpha 3n)$ was eliminated by performing control experiments: a lead target was bombarded by accelerated neon nuclei. No fissioning products with half-lives on the order of a minute were observed in a wide range of ^{22}Ne energies in the reactions $^{208}\text{Pb}(^{22}\text{Ne}, 3n)$ and $^{208}\text{Pb}(^{22}\text{Ne}, 4n)$. Thus, the reactions $^{209}\text{Bi}(^{22}\text{Ne}, p2n)$ and $^{209}\text{Bi}(^{22}\text{Ne}, p3n)$ should not be accompanied by fission fragments. Fission was also not detected in the bombardment of ^{209}Bi by ^{18}O ions of energy sufficient for occurrence of the reaction $^{209}\text{Bi}(^{18}\text{O}, 3n)$, thus eliminating the possible appearance of fissioning products in the reaction $^{209}\text{Bi}(^{22}\text{Ne}, \alpha 3n)$. The set of experiments performed made it possible to identify the isotope accompanied by fission with half-life equal to 60 sec as ^{228}Np . The cross section for producing fissile nuclei at the maximum of the excitation function of the reaction $^{209}\text{Bi}(^{22}\text{Ne}, 3n)$ was $0.45 \times 10^{-33} \text{ cm}^2$. All the neutron-deficient nuclei that we synthesized were odd-odd (^{228}Np , $^{232,234}\text{Am}$). This fact, as mentioned above, favors the occurrence of delayed fission.

Later on, in 1972, a careful analysis of these experiments was performed.¹⁴ It was thereby definitely established that the observed fragment activities were due to fission from an excited state of the daughter nuclei produced after EC decay of the parent nuclei $^{232,234}\text{Am}$ and ^{228}Np . The authors also showed that the energy Q_{EC} of EC of ^{228}Np and ^{232}Am is larger than the fission barriers B_f of the daughter nuclei ^{228}U and ^{232}Pu , while for ^{234}Am the value of Q_{EC} is comparable to B_f of ^{234}Pu . The probabilities P_{DF} were estimated as $\sim 10^{-3}$ for ^{228}Np and 10^{-2} for ^{232}Am , and a relation between P_{DF2} for ^{232}Am and P_{DF4} for ^{234}Am was found: $P_{\text{DF2}} > P_{\text{DF4}}$.

Thus, in heavy-ion beams we had synthesized the parent nuclei ^{228}Np , ^{232}Am , and ^{234}Am , whose daughter products arising after EC, ^{238}U , ^{232}Pu , and ^{234}Pu , undergo fission from an excited state.

The half-lives of the parent nuclei with respect to EC on the order of minutes and the relatively large production cross sections made these nuclei the primary objects of further study of the delayed fission of neutron-deficient nuclei by radiochemical methods. It was directly confirmed that nuclides with half-lives in this range undergo delayed fission, although by that time the available indirect data left no doubt about the nature of the process.^{15–17} It should be noted that in the study by Sommerville *et al.*,¹⁸ which appeared in 1977 and partially verified our experiments (the existence of the 2.6-min activity and the minute half-life of the ^{228}Np isotope were confirmed), doubt was expressed regarding our proposed interpretation of the observed fission as delayed fission. However, experiments to seek and identify delayed fission of nuclei with $N < 126$ definitively resolved the nature of the processes leading to the fission of products of neutron-deficient nuclei.

2.2. Synthesis and study of the nuclides ^{234}Am and ^{232}Am in nuclear reactions in accelerated beams of α particles

The delayed fission of ^{234}Am and ^{232}Am in nuclear reactions involving accelerated α particles has been studied in detail. This is due to the relatively long half-lives of these isotopes, which make it possible to use complicated techniques such as the chemical separation of elements. The latter made it possible to purify, to a great extent, americium from the γ activities which make it difficult to detect the x rays accompanying K capture in daughter plutonium nuclei. Chemical purification and separation of elements became an important factor allowing the measurement of coincidences of fission fragments with x-ray emission from daughter nuclei, and also the measurement of σ_{EC} , the cross section for production of isotopes undergoing K capture, and P_{DF} , the delayed-fission probability.

Habs *et al.*¹⁹ were the first to synthesize ^{232}Am in beams of α particles of energy 104 MeV in the nuclear reaction $^{237}\text{Np}(\alpha, 9n)^{232}\text{Am}$. In the bombardment of a target $100 \mu\text{g}/\text{cm}^2$ thick, recoil nuclei were ejected from the target and decelerated in a thin graphite film ($100 \mu\text{g}/\text{cm}^2$) placed 5 mm beyond the target. After switching off the accelerator beam, the collector film was moved by means of a tube conveyor into the gap between two surface-barrier detectors located 60 cm from the target. Habs was the first to use this detection method in studies of delayed fission.

The small thickness of the graphite film allowed the fission fragments and α particles of nuclear-reaction products to be recorded. The decay curve of fissioning nuclei identified as the product of ^{232}Am transformations was measured. The effect on the result of the decay of other nuclei which could be produced in parallel reactions was taken into account according to various considerations. For example, if it was assumed that an observed decay was associated with the synthesis of ^{228}Np nuclei, then the probability for the delayed

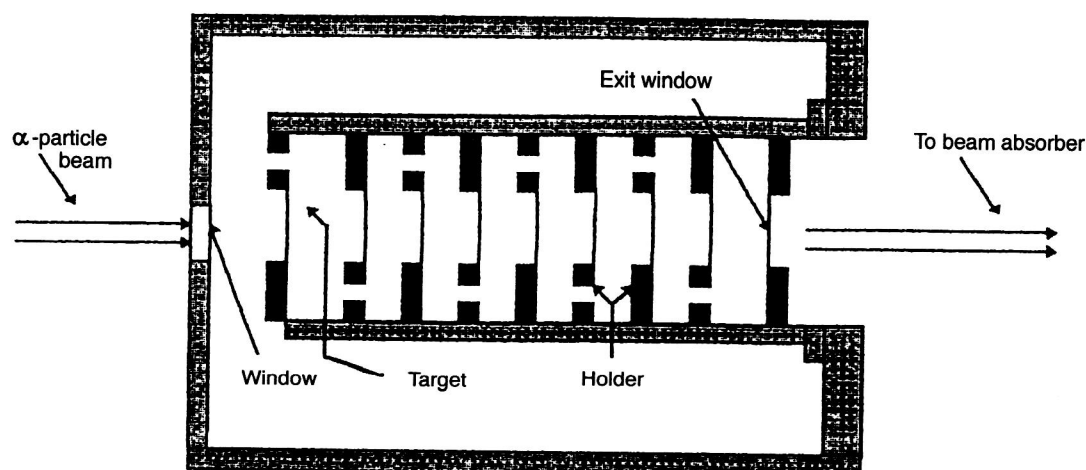


FIG. 9. The multiple-target assembly. Nine targets located along the beam axis of the bombarding particles beyond the beryllium entrance window are shown (in actual experiments their number reached 23). The helium flow with KCl aerosols absorbing recoil nuclei decelerated in the helium pass through the spaces behind each target and transfer the synthesis products to collectors, either on a disk (Fig. 10) or at a chemical laboratory.

fission of this nucleus obtained from the experimental data turns out to be several orders of magnitude higher than that found in Refs. 1 and 18. The synthesis of ^{231}Pu also could not affect the results. If the source of the fragments were the ^{231}Pu isotope, then its delayed-fission probability P_{DF} would reach $\sim 8\%$, from which it would follow that its half-life is of order 10^3 min. The latter contradicts the known values of the half-lives of neighboring isotopes, which typically have $T_{1/2} \sim 10^{10}$ yr. Other nuclei were excluded on the basis of analysis of the results of Ref. 3.

The characteristics of the α decay of the ^{232}Am isotope were measured by coincidences of α particles from this nucleus with the α decay of the daughter nuclei, whose half-lives fall in the microsecond range. The ratio of the probabilities for α decay and EC decay was estimated with an accuracy of up to 50%. The cross section $\sigma_{\text{EC}} = (0.4 \pm 0.7) \times 10^{-30} \text{ cm}^2$ was calculated from the data on the yield of α -active nuclei and the cross section for ^{232}Am production. The discrepancy between the half-life of ^{232}Am and the values measured in heavy-ion reactions is due to the small statistics and the different type of background in experiments using heavy-ion and α -particle beams. However, the discrepancy lies within the experimental errors.

A great advance in the study of delayed fission was the development by Hall *et al.*^{7,20} of a method combining fast transfer of nuclear-reaction products by an aerosol flow in a helium medium²⁰ and a multiple-target assembly (first used by Gangrskii and coworkers²²). The multiple-target assembly with transport of nuclear-reaction products by aerosols in a helium medium (see Fig. 9) was used by Hall *et al.*²⁰ for a comprehensive study of the delayed fission accompanying the parent nuclei ^{234}Am and ^{232}Am . Sections 2.3–2.7 below are devoted to describing these studies.

The ^{234}Am nuclei were synthesized by using accelerated α -particle beams at the 88-inch cyclotron at the Lawrence Berkeley Laboratory.²⁰

A drawback of studies performed in beams of deuterons, ^3H , and α particles, when the nuclear products are accumulated by a collector, is the need to bombard a fairly thin target, so that the mean free path of a synthesized nucleus

with small momentum obtained from a light particle exceeds the thickness of the target layer. The use of the multiple-target assembly eliminates this defect and makes it possible to obtain a very high yield of americium isotopes in a beam of accelerated α particles. This is achieved by placing many targets along the axis of the accelerated α -particle beam with a thin layer of bombarded material in each target. The ^{237}Np isotope is most suitable for synthesizing ^{234}Am and ^{232}Am in beams of accelerated helium ions. It was employed as the material in the first experiments using 12 targets on a molybdenum backing of thickness $2.5 \mu\text{m}$ with neptunium content ranging from 150 to $250 \mu\text{g}$. The area of each target was 1.23 cm^2 . The measured target thicknesses ranged from 125 to $200 \mu\text{g/cm}^2$. The targets were located sequentially along the beam axis with $\sim 1 \text{ cm}$ spacing. A beryllium foil of thickness $25 \mu\text{m}$ served as the entrance window, and another identical foil served as the vacuum window of the target system. The first experiments showed that the molybdenum backings were strongly activated, and so they were replaced by beryllium ones. In the bombardment of ^{237}Np by accelerated α particles, the intensity of the delayed-fission fragments, other conditions being equal, was proportional to the number of simultaneously bombarded targets. An accelerated α particle should pass through a thin target with a small energy loss. In this case, identical nuclear reactions will occur in all the targets. Moreover, if a nuclear reaction with a heavy nucleus occurs in one of the targets, its products will possess momentum sufficient to leave the thin target layer. In the Hall experiments, up to 23 targets were bombarded simultaneously.

The recoil nuclei were decelerated in helium and captured by KCl aerosol. The helium flow was carried away from the space behind each target by the aerosol to a chlorovinyl capillary tube which transferred the reaction products either to a collector film attached to a rotating disk or to a catcher foil, which was then sent to a chemical laboratory.

In addition to the efficient use of the α -particle beam, the multiple-target assembly also has another important advantage: the targets are located close together, and they absorb the fission fragments emitted from them. As a result, the

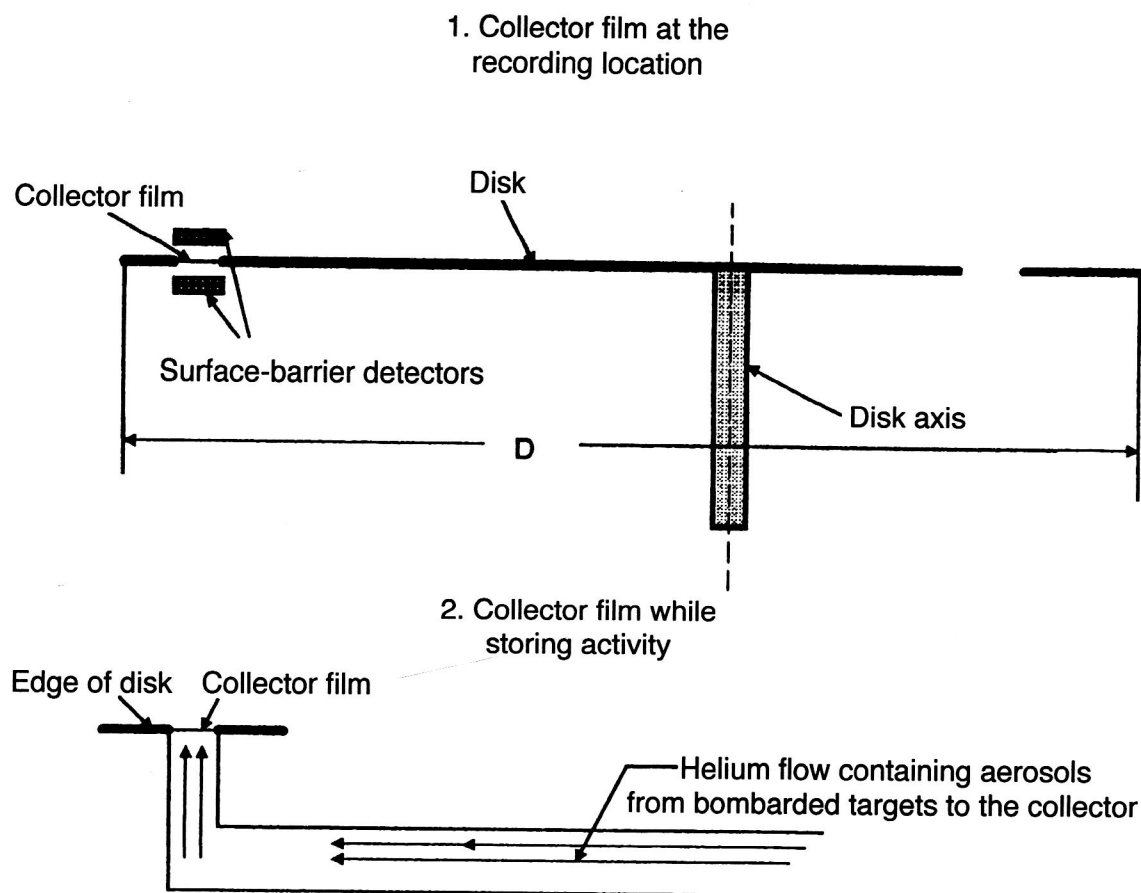


FIG. 10. At the periphery of the disk there are 80 collector films to catch aerosols containing reaction products and six pairs of surface-barrier detectors located opposite each other, between which the disk of collector films containing the studied activity captured by the aerosols rotates.

aerosols transferred to the detectors are not contaminated by fragments.

To measure the characteristics of the fission reaction $^{234}\text{Am} \rightarrow ^{234}\text{Pu} \rightarrow \text{ff}$, the aerosols containing nuclear-reaction products were transported to a distance of ~ 5 m and collected by a polypropylene collector film of thickness $\sim 40 \mu\text{g}/\text{cm}^2$ located on the periphery of a disk. The disk was moved with a stop every 4.5° , so that the collector film containing the nuclear-reaction products ended up between two silicon surface-barrier detectors (SSBDs) located above and below the disk plane (see Fig. 10). There were six pairs of such detectors altogether along the disk. A disk contained 80 collector films. When ^{234}Am nuclei were studied, the exposure time was 2.5 min at all the measurement positions. Each collector film occupied six positions between each pair of detectors. Fission fragments and α particles were recorded. The efficiency of recording coincident fission fragments was 60%, and was the same for α particles.

The first location of the collector film was in front of the nozzle feeding aerosol into it from the multiple-target assembly. The collector moves from this position to the first recording position between two SSBDs. It is only here that the detection of α particles is delayed by 12 sec in order to avoid background from products of reactions occurring in the target backing (fragments are recorded continuously). Each collector successively passes through all six detection positions, with the emissions being measured for six collectors simul-

taneously. After the sixth position their activity is not measured. Thus, the activity is accumulated on a single collector, while recording is done on the other six. The resolution in the α -particle energy is 40 keV. Each disk has 80 collectors. After a complete rotation of the disk, which takes about 3 h and 20 min, it is replaced, thereby eliminating the background from stored, long-lived, spontaneously fissioning activities which could introduce errors into the subsequent measurements. In all the experiments, 1188 coincident pairs of fission fragments were recorded. According to these data, the half-life was $T_{1/2} = 2.32 \pm 0.08$ min. This quantity is practically the same as the value measured earlier,¹ 2.6 ± 0.2 min, when the measurement errors are taken into account.

The observed fission cross section in the reaction $^{237}\text{Np}(\alpha, 7n)$ was estimated on the basis of analysis of the decay curve. If the thickness of each target is taken to be $75 \mu\text{g}/\text{cm}^2$ and the efficiency of the aerosol collection system is 100%, then this cross section will be $\sim 0.2 \times 10^{-33} \text{ cm}^2$.

The technique used for ^{232}Am was practically the same.⁷ The half-life of the fragment activity was obtained by bombarding a ^{237}Np target by α particles of energy 99 MeV. In the detection of fragments from the delayed fission $^{232}\text{Am} \rightarrow ^{232}\text{Pu} \rightarrow \text{ff}$, 2201 coincidences were recorded. The half-life of ^{232}Am turned out to be 1.31 ± 0.04 min, in agreement with the results obtained in earlier studies (see, for example, Ref. 3) and differing considerably from the value

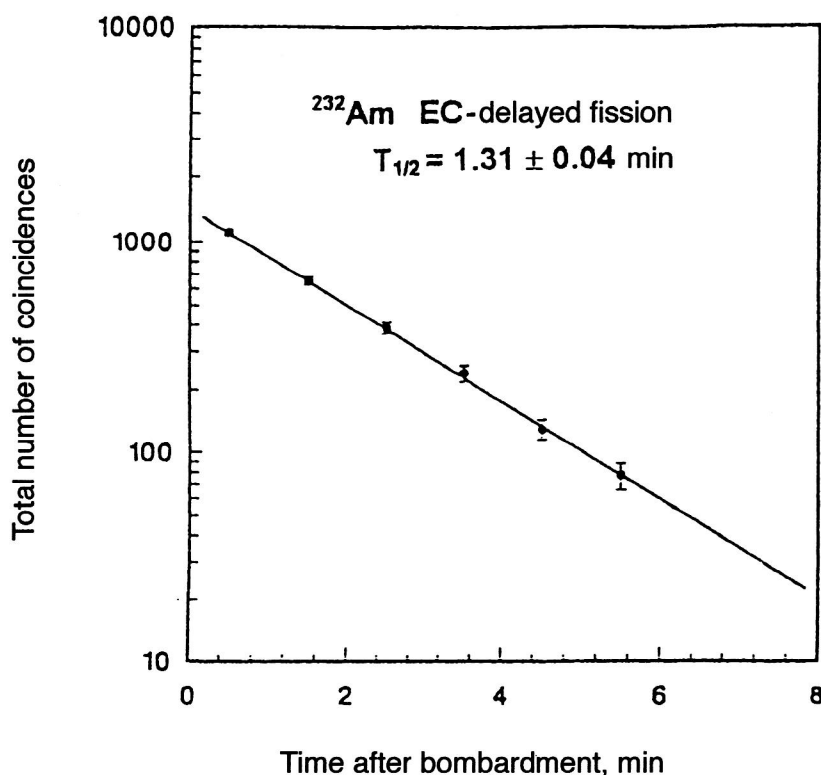


FIG. 11. Decay curve for the chain $^{242}\text{Am} \rightarrow ^{232}\text{Pu} \rightarrow \text{ff}$, constructed from the number of recorded coincidences of fission fragments. The setup of Fig. 10 was used. The collector was located at each position between SSB detectors for 1 min.

given by Habs *et al.*¹⁹ The decay curve is shown in Fig. 11. The cross section for production of fissile ^{232}Pu was $\sim 2.5 \times 10^{-33} \text{ cm}^2$ according to the Hall measurements.

Two chemical techniques were used in the chemical laboratory to separate nuclear-reaction products. The first technique was designed to determine whether the source of the fissile product in the reaction $^{237}\text{Np}(\alpha, 7n)$ or $^{237}\text{Np}(\alpha, 9n)$ belonged to an element with a given atomic number, namely, americium. Since the atomic number Z of all the products of these reactions was ≤ 95 , it is sufficient to separate americium only from actinides with $Z < 95$. Americium is the only trivalent actinide produced in $^{237}\text{Np}(\alpha, xn)$ reactions, and a simple anion column separates it from actinides with smaller atomic number. It was not necessary to remove the fission products in order to identify the atomic number.

The second technique was used to purify the americium from fission fragments which could produce background making it difficult to detect x rays from the daughter plutonium nucleus appearing in the population of the freed vacancy of the K electron during the transformation of the parent nucleus into the daughter nucleus.

Measurement of x rays in coincidence with delayed-fission fragments allows the experimental measurement of the delayed-fission probability P_{DF} , and the main achievement of this experiment was the direct proof that delayed fission actually occurs.

2.3. Identification of the atomic number of an element

In this subsection we discuss the technique for the radiochemical identification of the americium fraction containing

the $^{232,234}\text{Am}$ isotopes—the predecessors of delayed fission.^{7,20} Their half-lives and production cross sections have been measured.

The nuclear-reaction products collected during 3 min after the bombardment of a ^{237}Np target by α particles of energy 75 MeV were separated in ion-exchange columns. In the americium fraction 27 fissions were observed, while in the neptunium–plutonium fraction only a single one was seen. The latter was consistent with possible contamination of the neptunium–plutonium fraction by tails of americium containing the isotope ^{234}Am . (Control experiments gave $\sim 2\%$ for the mutual contamination of the fractions.) The chemical procedures took only 90 sec.

In the americium fraction, α radiation of energy 6.46 MeV was recorded. Francium, radium, and actinium, lanthanides in the separation for the types of resin used, follow americium. However, these elements (observed in the α spectra) are produced in negligible quantities in nuclear reactions occurring in the bombardment of a ^{237}Np target by α particles, and lanthanide nuclei do not undergo fission. The fragments could therefore only be the product of the delayed fission $^{234}\text{Am} \rightarrow ^{234}\text{Pu} \rightarrow \text{ff}$.

2.4. Measurement of coincidences of fragments from delayed fission and x rays from K capture

The time correlations between the x rays accompanying K capture in the nuclei ^{234}Am and ^{232}Am and the fragments following the delayed fission of ^{234}Pu and ^{232}Pu were measured from their activity in collectors using aerosols without the chemical-separation stage.^{7,20,23} A tantalum foil with aerosols containing the activity under study and an SSBd of area 300 mm^2 located in front of it were placed between two

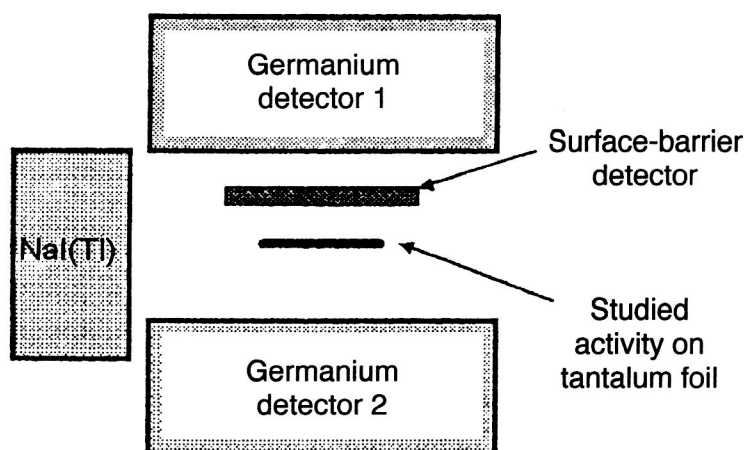


FIG. 12. Location of the detectors in the setup to record correlations of fission fragments and x rays in the process $^{234}\text{Am} \rightarrow ^{234}\text{Pu} \rightarrow \text{ff}$.

germanium γ detectors. The measuring apparatus also included a NaI(Tl) γ detector allowing the best time resolution to be obtained (see Fig. 12). The calibration was done by using K x rays of curium in coincidence with the α particles of the parent nucleus ^{249}Cf . The efficiency of recording the x rays in the plutonium region was estimated to be 9%. Measurements of coincidences of prompt γ rays with fission fragments from ^{252}Cf made it possible to determine the total efficiency of detecting the K radiation of ^{232}Pu in the delayed fission of ^{232}Am . This turned out to be $\sim 12\%$.

In a fission of a nucleus with small excitation energy in the americium–californium region, the fragments emit about 10 γ rays.²⁴ The γ detectors receive a high load. Owing to the superposition of the x-ray and prompt- γ pulses of the fragments, some of the x rays of ^{234}Pu or ^{232}Pu do not fill up the x-ray photopeak. The superpositions can largely be eliminated by decreasing the number of recorded γ rays. However, this leads to a decrease of the x-ray detection efficiency and, consequently, the degree to which a correlation is observed. In the end, it proved possible to optimize the process of recording correlations of fission fragments and x rays. The distance between the γ detectors and the foil containing the activity was fixed in such a way that the level of x rays unobserved owing to coincidences with prompt emission of fission fragments was minimized. In the process of measuring the coincidences of prompt γ rays with fragments from the spontaneous fission of ^{252}Cf , the distance between the γ detectors and the target containing ^{252}Cf was selected to be optimal for recording, because the numbers of prompt γ rays produced per fission of americium or californium are practically the same. The level of unrecorded x rays was no more than 50%. Each detector covered a solid angle of $\sim 6.7\%$ of 4π .

In order to study coincidences of x rays and fission fragments of the isotope ^{234}Pu , the activity of the products of the reaction $^{237}\text{Np} + ^4\text{He}$ at energy of the bombarding α particles corresponding to the excitation function of the reaction $^{237}\text{Np}(\alpha, 7n)$ was stored in collectors during a time of 4 min, using a gas jet. Then the activity was moved to the measurement chamber.

The rate of counting γ rays was $\sim 10^3 \text{ sec}^{-1}$. The probability for random coincidences of fission fragments and γ

rays was less than 0.10% because the width of the time window was small. It was subsequently decreased to 0.01%. In Fig. 13 we show the x rays and γ spectra of coincidences with signals from fission fragments.

By statistical processing of the data, the most probable energy of the $K\alpha_1$ line turned out to be $103.6 \pm 0.5 \text{ keV}$, in excellent agreement with the tabulated value of the $K\alpha_1$ energy of plutonium, equal to 103.76 keV (Ref. 24). The detection of x rays from plutonium implied that the lifetimes of states in the potential well from which the fission occurs are larger than or of the same order as the time $\sim 10^{-17} \text{ sec}$ needed for the orbital electrons to populate the vacancy in the atomic K shell.²⁵ The lifetime τ of the excited state of the ^{234}Pu nucleus must lie in the range $10^{-17} < \tau < 3 \times 10^{-9} \text{ sec}$.

If the nucleus is actually delayed in the second potential well of the fission barrier, then the lifetime of the shape isomer ^{234f}Pu also lies in this range. These values are consistent with the systematics of the shape-isomer lifetimes of plutonium,²⁷ from which it follows that the half-life $T_{1/2}$ of the shape isomer ^{234f}Pu lies in the range from 10^{-8} to 10^{-12} sec .

For the daughter product of the parent nucleus ^{232}Am produced after EC, the measured data give the most probable value $K\alpha_1 = 103.8 \pm 0.3 \text{ keV}$, which practically coincides with the tabulated value of the $K\alpha_1$ energy of plutonium.

The lifetimes of excited states of ^{232}Pu were estimated just as for ^{234}Pu . They lie in the range from 10^{-8} to $8 \times 10^{-9} \text{ sec}$. This implies that the lifetime of the shape isomer ^{232f}Pu lies in this range. The lifetime systematics of spontaneously fissioning shape isomers gives $(1-10) \times 10^{-12} \text{ sec}$ for ^{232f}Pu .

The curves representing the γ coincidence spectra contain six weak photopeaks in the energy range 77–283 keV. Prompt γ rays from fission fragments do not produce such a structure. It is not impossible that these photopeaks reflect the structure of the levels in the second potential well of the ^{232}Pu isotope. If this is so, a new possibility for studying shape isomers is revealed.

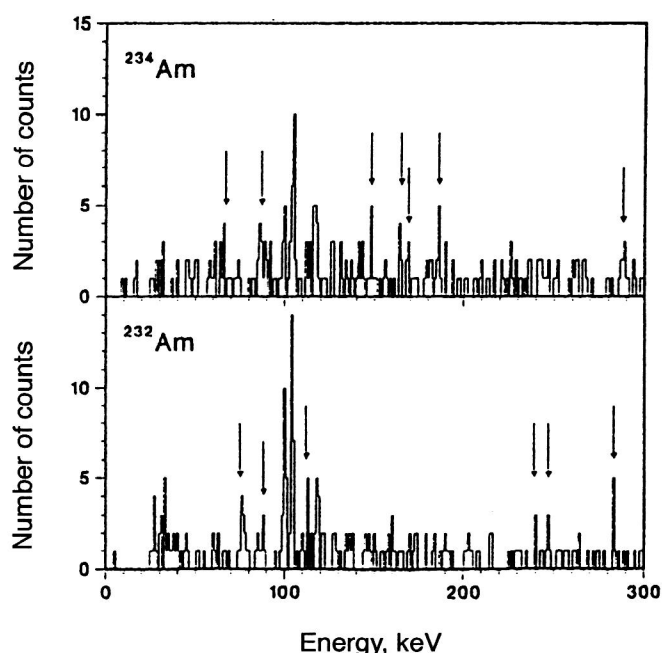


FIG. 13. Spectra of x rays and γ radiation in coincidence with fragments from the delayed fission after EC of ^{232}Am and ^{234}Am . The anomalous background peaks may be due to γ transitions in the second potential well. They are indicated by the arrows.

2.5. The total kinetic energy of fragments of the ^{232}Am and ^{234}Am isotopes and the fragment mass distribution

The high intensity of delayed-fission fragments observed in Refs. 7 and 20, owing to the use of the multiple-target assembly with aerosol transport of nuclear-reaction products (in contrast with experiments with a single target), made it feasible to measure the total kinetic energy (TKE) of the fission fragments and their mass distribution in delayed fission with the predecessors ^{232}Am and ^{234}Am [$^{232,234}\text{Am}(\text{EC}) \rightarrow ^{232,234}\text{Pu}(\text{f}) \rightarrow \text{ff}$].

These characteristics are of particular interest in connection with the considerable distance of the isotopes ^{232}Pu and ^{234}Pu from the β -stability line and the fission of these isotopes from states with low excitation energy. The authors hoped that study of the $^{232,234}\text{Pu}$ fragment distributions would make it possible to understand the processes associated with the thorium anomaly and other features of the fission of heavy nuclei far from the β -stability line, and of the total kinetic energy and mass distribution of the fission fragments in the transformation chain $^{234}\text{Am}(\text{EC}) \rightarrow ^{234}\text{Pu}(\text{f}) \rightarrow \text{ff}$. The measurement of these characteristics is of particular interest in connection with the fairly large distance of the ^{234}Pu isotope from the β -stability line, and also the fission of this isotope from states with low excitation energy. The distribution of fission fragments from the daughter isotope ^{234}Pu is strongly asymmetric. Roughly from 1000 to 2000 fission events were recorded in the experiments. This made it possible to measure the fission characteristics with high accuracy.

In the final analysis, these measurements, together with the work of Gangrskii *et al.*,⁶ showed that delayed fission after EC is characteristic of neutron-deficient actinide nuclei.

In Table I we list the characteristics of the fission of ^{232}Pu and ^{234}Pu produced in the delayed fission after EC of the predecessors ^{234}Am and ^{232}Am .

The distribution of the fragment yield as a function of the TKE is symmetric about the maximum and contains only one component. The average value of the TKE for ^{234}Pu fission fragments is 175 MeV, and close to the value predicted for fission from the ground state.^{27,28}

The TKE distribution is symmetric about the energy 174 MeV for fragments from the delayed fission after EC $^{232}\text{Am} \rightarrow ^{232}\text{Pu} \rightarrow \text{ff}$ and practically coincides with the measured TKE of the fragments from the delayed fission of ^{232}Pu .

The method of delayed fission significantly extends the region of neutron-deficient nuclei whose fission characteristics can be studied. For example, for nuclei like ^{232}Pu and ^{234}Pu , the partial half-lives with respect to fission from the ground state are too large compared with the overall half-lives, so that study of fission is impossible.

2.6. Study of the α decay of ^{234}Am and ^{232}Am

The study of the α decay of light americium nuclei is interesting for determining the value of the α branch in de-

TABLE I. Mass and energy distributions of fission fragments from the nuclei ^{234}Pu and ^{232}Pu .

Nucleus	^{234}Pu	^{232}Pu
TKE after neutron emission	171 ± 5 MeV	173 ± 5 MeV
TKE before neutron emission	173 ± 5 MeV	174 ± 5 MeV
KE of fragments with high energy	98.6 ± 2.0 MeV	99.4 ± 1.9 MeV
KE of fragments with low energy	72.3 ± 1.5 MeV	73.6 ± 2.0 MeV
KE ₁ of fragments with high energy	99.4 ± 2.0 MeV	100.2 ± 1.9 MeV
KE ₁ of fragments with low energy	72.9 ± 1.5 MeV	74 ± 2.0 MeV
Average mass of light fragments	99.0 ± 0.1	98.7 ± 0.3
Average mass of heavy fragments	135.0 ± 0.1	133.3 ± 0.3

Here TKE is the average total kinetic energy of the fission fragments, KE is the average kinetic energy of a fission fragment after neutron emission, and KE₁ is the average kinetic energy of a fragment before neutron emission.

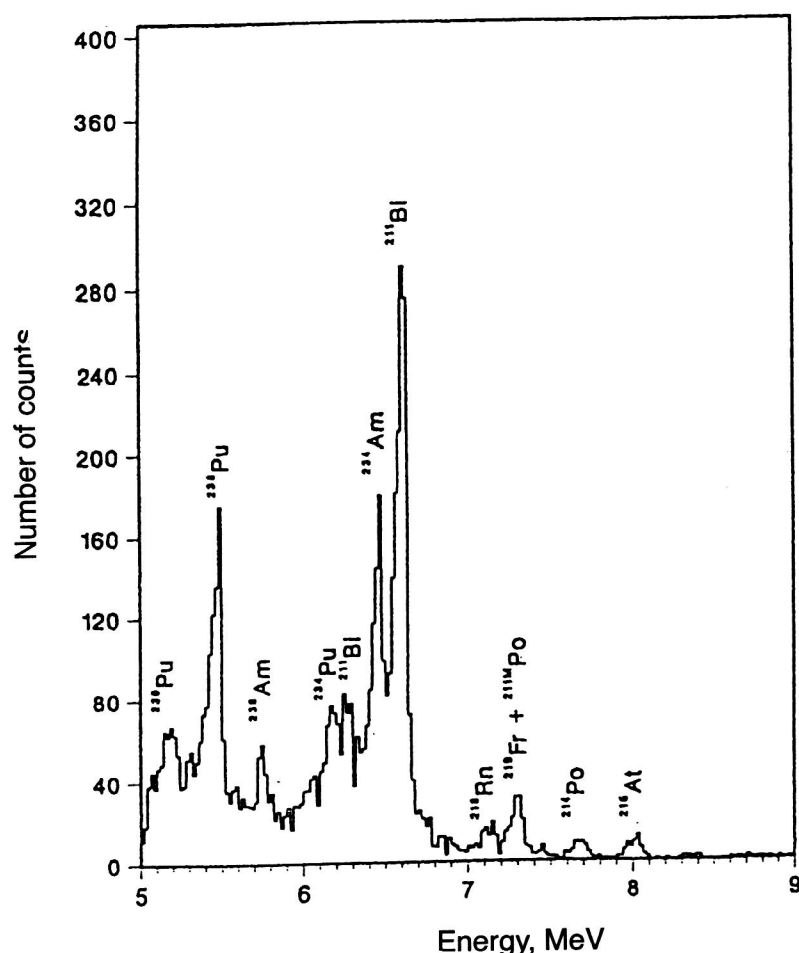


FIG. 14. Alpha spectrum of the products of $^{237}\text{Np}(\alpha, xn)$ reactions in study of the ^{234}Am isotope. The measurements were performed at a setup with a rotating disk (Fig. 10) at the second detector position. The exposure time was 2.50 min.

layed fission. As shown below (see Sec. 2.9), for nuclei with $N < 126$ it is α decay which determines the possibility of detecting delayed fission. It is therefore also important to study its effect on the predecessors in delayed fission after EC, ^{234}Am and ^{232}Am .

In Fig. 14 we show the α spectrum of the products of the reaction $^{237}\text{Np} + ^4\text{He}$. The peaks of the α emitters produced in parallel reactions with ^{234}Am and reactions with lead and bismuth impurities, which as a rule are present in the target, are clearly seen. The high intensity of the β emission makes it impossible to use the first position of the collector on the disk to study α decay.

The peak with α -particle energy 6.46 MeV includes two activities: one with half-life of about 2.3 min, and the other with a very long half-life which could not be measured under the experimental conditions. The time 2.32 min was associated with ^{234}Am decay. The long-lived activity presumably belongs to the tails of ^{211}Bi formed after the β decay of ^{211}Pb .

Comparison of the initial activities of the α - and EC-decay branches gives the ratio α -decay/fission = 5.8 ± 0.4 . On the basis of the earlier assumptions about the efficiency of the activity transfer by KCl aerosols in a helium flow and the data on the effective target thickness, the lower limit on the partial cross section for ^{234}Am production was found to be $1.1 \times 10^{-33} \text{ cm}^2$. The α -decay branch of ^{234}Am amounted to an insignificant fraction: $(3.9 \pm 1.2) \times 10^{-4}$.

It was not possible to measure the α branch of ^{232}Am in the background of the α emission from products produced on targets not containing lead and bismuth impurities near the expected α -particle energies.

2.7. Experimental measurement of the delayed-fission probability P_{DF} and the cross section σ_{EC} for production of a nucleus undergoing K capture

The experimental measurement of P_{DF} requires measurement of the ratio of the number of delayed-fission fragments and the total number of ECs in a given time interval. Direct measurements of P_{DF} are difficult because charged particles are not emitted in EC, and the EC branch leads to long-lived nuclei which decay in the same way. The EC branch can be measured only by recording x rays. Therefore, in this case it is necessary for the americium to be highly pure in order to avoid contamination from fission fragments creating intense γ background.

A column of two types of ion-exchange resin was used for this. The column of dimension 3 mm \times 10 mm was loaded with cation-exchange resin and then with anion-exchange resin. The anion-exchange resin was therefore located at the top. Washing with concentrated HCl separates americium from monovalent and divalent fission products and lanthanides in the upper part of the column, and then plutonium and neptunium are absorbed in its lower part.^{7,20}

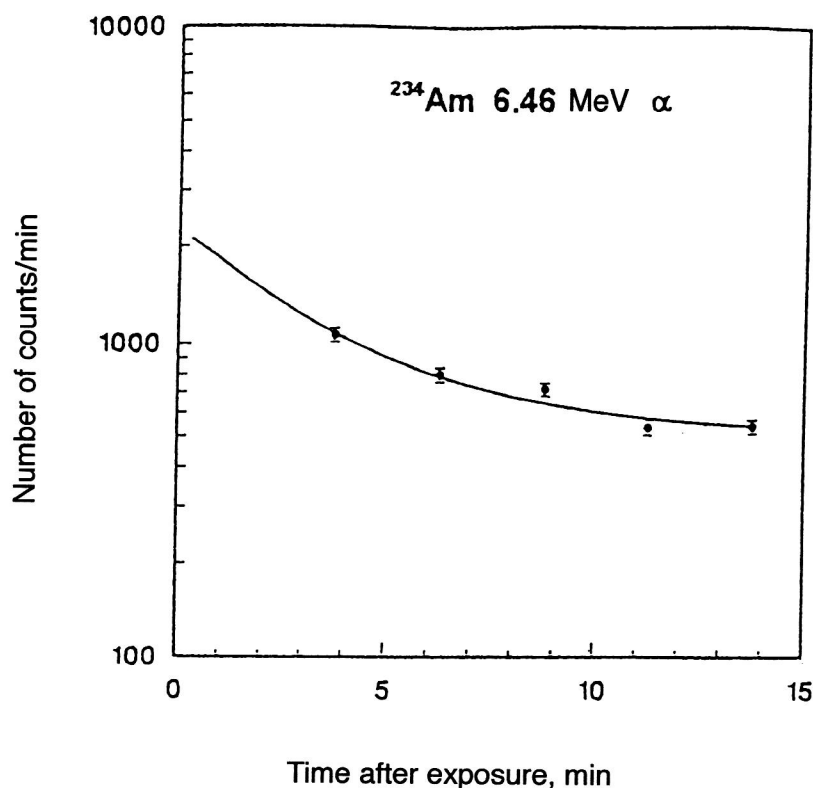


FIG. 15. The α -decay curve of an isotope of the α group with energy 6.46 MeV (^{234}Am).

The elements were separated in a chemical laboratory, where the activity from the targets was transported through a distance of 80 m to a collector. KCl salt containing the captured activity was dissolved in 20 mm³ of 0.5 mol HCl. The isotope marker ^{241}Am ($T_{1/2}=432$ yr) was added to the solution to monitor the yield. The solution was then passed through the column. The americium from the column was washed with concentrated HCl. Then the americium fraction was coprecipitated along with CeF_3 . After filtering and washing, the precipitate was placed in a γ spectrometer containing germanium detectors (see Fig. 12). It took about four minutes to perform all these chemical operations.

The same chemical separation of elements was also used in studying ^{232}Am , except for one difference: the stage of coprecipitation with CeF_3 was omitted in the experiments recording x rays from ^{232}Pu . The time for the chemical procedures was therefore decreased from 4 min to 90 sec.

Fission in the chain $^{234}\text{Am} \rightarrow ^{234}\text{Pu}$ was studied by a different method, using samples obtained by the same aerosol collection as in the earlier experiments, but without any chemical procedures. After thermal processing, tantalum foil containing the activity was placed inside a proportional counter with a gas flow. The exposure time was 10 min, sufficient to measure the total number of fissions in the collected active material. The efficiency of recording fission was 98.6%.

The americium fractions were periodically separated during the four-hour bombardment. The characteristics of the nuclear fission were measured simultaneously with the chemical separation. Every 40 minutes the γ radiation of chemically cleaned americium was recorded. The fragment activities were placed inside a proportional counter for 10

min each. In Fig. 15 we show the characteristic γ spectrum. The decay of the ^{237}Am and ^{238}Am isotopes synthesized in nucleon-transfer reactions was recorded. Peaks from the decay of nuclei which are the products of reactions with the target backing and mounting are also clearly seen.

The γ energy characteristic of x rays from americium contains a peak consisting of two components: a short-lived one with half-life 2.3 min, and a long-lived one with $T_{1/2} \sim 1$ h. The long-lived component is a mixture of ^{237}Am ($T_{1/2}=73$ min) and ^{238}Am ($T_{1/2}=1.63$ h), and the short-lived one is associated with ^{234}Am .

The EC-decay constant of ^{234}Am was used to calculate σ_{EC} and P_{DF} . The cross section σ_{EC} was determined by using the following data. The total thickness of all 12 targets was 0.90 mg/cm², and the aerosol transfer of the activity is conventionally assumed to be 100%. It was assumed that the level density of the daughter nucleus is high, so that the excitation is removed by a cascade of high-energy transitions (500–1000 keV) with small multipole order. Therefore, the possibility of producing K x rays due to internal conversion was not taken into account. As a result, σ_{EC} was found to be $5.4 \pm 1.3 \mu\text{b}$. The probability P_{DF} was calculated on the basis of the initial EC activity and the number of recorded fission fragments. By measuring each of these quantities practically simultaneously, the effect of small changes in the parameters of the experimental setup was eliminated. Thus, P_{DF} can be calculated by using the equation

$$P_{\text{DF}} = \lambda \frac{I_f}{[e^{-\lambda t_1} - e^{-\lambda(t_1+t_2)}] D_{\text{OBC}}}. \quad (12)$$

Here λ is the decay constant of ^{234}Am , I_f is the number of

fissions in the counting time t_2 , t_1 is the time interval from the end of the bombardment to the start of the fragment counting, and D_{OEC} is the initial EC activity. The delayed-fission probability was calculated for all the measurements. Its average value was $(6.6 \pm 1.8) \times 10^{-5}$. The ratio of the α -decay probability and the fission probability was $(3.9 \pm 1.2) \times 10^{-4}$.

A similar method was used for the ^{232}Am isotope.²³ The x rays emitted in population of the K shell of ^{232}Pu were measured. The fission fragments and their energy were recorded by a windowless proportional counter. The x-ray emission of the daughter ^{232}Pu nucleus is weak, but clearly distinguishable. Two half-lives were observed: 1.31 min (^{232}Pu) and ~ 1 h (a mixture of ^{237}Am and ^{238}Am). The cross section is $\sigma_{\text{EC}} = (1.3 \pm 0.2) \times 10^{-30} \text{ cm}^2$. The delayed-fission probability is $\sim 10^{-4}$. The latter value differs by 1.3–2 orders of magnitude from the values of earlier studies.¹⁹

The resulting values of the lower limit on the cross sections and the decay branches are $\sigma_{\text{EC}} > 1.3 \times 10^{-30} \text{ cm}^2$, $\sigma_{\text{EF}} > 2.5 \times 10^{-33} \text{ cm}^2$, $P_{\text{DF}} = (6.9 \pm 1.0) \times 10^{-4}$, and $T_{1/2} = 1.31 \pm 0.04 \text{ min}$.

2.8. Study of the delayed fission of odd–odd isotopes with $Z > 96$

More complicated problems had to be solved in studying the delayed fission of transformation chains beginning with the parent neutron-deficient odd–odd berkelium, einsteinium, and mendelevium nuclei.

The isotopes ^{240}Bk , ^{242}Bk , ^{246}Es , and ^{248}Es were obtained by bombarding thick uranium and thorium targets with accelerated ^{14}N ions with a beam intensity of up to 10^{14} particles/sec.⁶ The active material was deposited on a slanted target located in the cyclotron chamber. Fission fragments were recorded by using polyethyleneterephthalate film of thickness $15 \mu\text{m}$. After etching the film in NaOH of optimal concentration, the fragment tracks were counted by means of an optical microscope. In some experiments the fission fragments were recorded by breakdown detectors. The operating principle of such detectors is based on the weakening of the dielectric strength of the film at the instant of passage of a fission fragment through it. If a large enough potential difference is applied to the film, breakdown occurs along the fragment track and is immediately recorded. The advantage of this method is that it can be used to measure fragment activity in real time.

When the energy of the nitrogen ions fell in the range 74–76 MeV, einsteinium and berkelium were synthesized in the nuclear reactions $^{238}\text{U}(^{14}\text{N}, 4n)^{248}\text{Es}$ and $^{232}\text{Th}(^{14}\text{N}, 4n)^{242}\text{Bk}$. These isotopes could be the parent nuclei of delayed-fission chains.

However, only single fission fragments were observed experimentally. Nevertheless, despite the small statistics, it was possible to estimate the ^{248}Es production cross section and to establish an upper limit on the delayed-fission probability.

Bombardment of ^{238}U and ^{232}Th targets by accelerated ^{14}N ions of energy in the range 92–94 MeV produced the maximum yield of fission fragments with the fragment time

distribution corresponding to the half-lives $8 \pm 2 \text{ min}$ and $5 \pm 2 \text{ min}$. The maxima of the excitation functions of the nuclear reactions $^{238}\text{U}(^{14}\text{N}, 6n)^{246}\text{Es}$ and $^{232}\text{Th}(^{14}\text{N}, 6n)^{240}\text{Bk}$ lie in the range 92–94 MeV, and the measured half-lives of the fragment activity are equal to the half-lives of the nuclei ^{246}Es and ^{240}Bk . This unambiguously indicates that the fission fragments belong to the daughter nuclei ^{246}Es and ^{240}Bk .

Owing to the small yield of fission fragments in these reactions, the understanding and elimination of possible sources of fragment background acquired special importance. For example, in the bombardment of a thick target, the level of fragment production due to fission of the target matter by prompt neutrons, hard γ rays emitted by prompt fragments, and γ rays from nuclei produced in the target backing was checked.

The results of control experiments showed that if the recording was begun ten minutes after the bombardment, the γ -ray background and the neutron background of prompt fission fragments do not introduce any errors into the data. It was noticed that the use of extremely pure aluminum as the target backing significantly reduces the γ flux and therefore lowers the background arising from the interaction of the target matter with the γ rays generated in the backing.

These experiments showed that in thick uranium and thorium targets the background exceeds the allowed level at which the study of delayed fission with production cross section $\sim 10^{-35} \text{ cm}^2$ and half-life of the order of 10 min can be studied. Therefore, the recoil nuclei ^{244}Es and mendelevium with mass numbers 248 and 250 were obtained from thin targets by collectors which transferred the reaction products to fission-fragment detectors. Here the target thickness ranged from 0.5 to 1 mg/cm^2 , and the heavy-ion current was less than 5 μA .

Gangrskii *et al.*⁶ obtained the time distributions of the yields of fissioning nuclei in the reactions $^{238}\text{U}(^{14}\text{N}, 5n)^{244}\text{Es}$ and $^{237}\text{Np}(^{12}\text{C}, 5n)^{244}\text{Es}$ at ^{14}N and ^{12}C energies of 82 MeV and 86 MeV, respectively. The half-life with respect to delayed fission is $T_{1/2} = 37 \text{ sec}$. Delayed fission with half-life $T_{1/2} = 52 \text{ sec}$ was observed in the reaction $^{243}\text{Am}(^{12}\text{C}, 5n)^{250}\text{Md}$. Comparison of the data on the yields of fissile nuclei and of the daughter nuclei ^{244}Cf and ^{250}Fm of isotopes formed after the EC of ^{244}Es and ^{250}Md allowed the delayed-fission cross section to be estimated. Delayed fission for nuclei with $Z > 95$ was observed with small statistics.

A group of authors have studied neutron-deficient delayed emitters by using heavy ions accelerated by the linear accelerator UNILAC (GSI, Darmstadt).³⁷ The recoil-nucleus velocity filter SHIP was used to separate the reaction products. The isotope ^{242}Es , the parent nucleus of the delayed fission after EC $^{242}\text{Es} \rightarrow ^{242}\text{Cf} \rightarrow \text{ff}$, was synthesized in the reaction $^{205}\text{Tl} + ^{40}\text{Ar}$. Three events were identified. The cross section for delayed fission was $\sigma_{\text{DF}} = 1.80 \times 10^{-34}$, and $P_{\text{DF}} = (1.4 \pm 0.8) \times 10^{-2}$. This value allows the barrier height in the fission of ^{242}Cf to be estimated as $\sim 5.4 \text{ MeV}$.

Later on, in studies using the same accelerator and velocity filter, in the reaction $^{209}\text{Bi}(^{40}\text{Ar}, 3n)^{246}\text{Md}$ it was found³⁰ that after the K capture of mendelevium, a stronger fission branch than what is possible only due to the contri-

bution of a single spontaneous fission of the daughter nucleus ^{246}Fm is formed. Therefore, the authors of that study attributed the additional yield of fission fragments to the delayed fission of ^{246}Md . These data gave $P_{\text{DF}} \sim 6.5 \times 10^{-2}$ for this nucleus. The accuracy of these data is poor, owing to the small number of observed events.

2.9. Delayed fission to the left of the neutron shell $N=126$ and in the region to the left of $Z=82$

As the neutron deficit grows in approaching the $N=126$ shell in the region of ultra-neutron-deficient nuclei, delayed fission is suppressed by the competing α decay. However, to the left of $N=126$ the α -decay energy Q_α falls off sharply and then slowly grows with increasing neutron deficit, the role of the α -decay branch is diminished, and the value of $T_\alpha/(T_\alpha + T_{\text{EC}})$ grows, which corresponds to enhanced competition of EC with α decay. Here the energy Q_{EC} already exceeds the fission-barrier height of the daughter nuclei, which are primarily even–even, and so it becomes possible to observe delayed fission.

The very first experiments to search for delayed fission after EC in the region of the filled nucleon shells with $N=126$ and $Z=82$ when $N < 126$ or $Z < 82$ were based on synthesis and study of the shell activity of the isotope ^{208}Ac at the Flerov Nuclear Reactions Laboratory. This experiment provided strong indirect evidence for the existence of a new type of radioactive decay—delayed fission. The appearance of such fissile isotopes was difficult to explain on the basis of other processes. As a result, in 1981 the delayed fission of the ^{208}Ac nucleus ($^{208}\text{Ac} \rightarrow ^{208}\text{Ra} \rightarrow \text{ff}$) was recorded (Refs. 15–17; see also Refs. 31 and 32). Therefore, the daughter fissioning nucleus already belonged to the class of preactinide nuclei.

A ^{197}Au target was bombarded by an intense beam of ^{20}Ne ions of energy up to 11 MeV/nucleon at the U-400 accelerator (a cyclotron with pole diameter 400 mm). The cross sections for producing fission activities fell in the range $(1.5\text{--}2.0) \times 10^{-35} \text{ cm}^2$. Thirty-five fission events were observed, and the half-life was estimated from their time distribution to be ~ 0.1 sec. The delayed-fission probability P_{DF} ranged from 10^{-1} to 10^{-3} . These studies opened up the remarkable possibility of studying nuclei 15–20 neutrons away from the β -stability line.

The barrier heights of the daughter even–even nuclei calculated by extrapolating the experimental data are given in Ref. 31. If the minimum cross section σ_f is taken to be 10^{-35} cm^2 , the threshold cross section σ_n for production of a neutron-deficient nucleus in the region of $Z < 126$ neutrons is given by $\sigma_n = [(T_\alpha + T_{\text{EC}})/(T_\alpha)](\sigma_f/P_{\text{DF}})$.

Nuclei in the vicinity of the $Z=82$ shell were studied in Ref. 33. In the bombardment of a ^{144}Sm target by ^{40}Ca ions of energy up to 230 MeV, the authors³³ discovered delayed fission with $T_{1/2} \sim 0.70$ sec, which they associated with the sequence $^{180}\text{Ti} \rightarrow ^{180}\text{Hg} \rightarrow \text{ff}$. By analyzing this transformation chain, the delayed-fission probability was estimated to be $P_{\text{DF}} \sim 10^{-6}$ (see Sec. 2.11, Table V).

2.10. Delayed fission of neutron-rich nuclei

Studies of delayed fission in the region of neutron-rich nuclei are of particular interest, since fission after β decay plays the main role in synthesizing heavy elements in the Universe, including the possible formation of superheavy elements near $Z \sim 114$ with a magic number of neutrons. The importance of delayed fission in nuclear nucleosynthesis was pointed out in Ref. 34.

Gangrskii *et al.*³⁵ studied the delayed fission of isotopes of protactinium with mass numbers 234, 236, and 238. The characteristics of odd–odd nuclei of these isotopes, the synthesis reactions, and the production cross sections are given in Table V.

The cross sections for reactions involving deuterons and neutrons at 14.7 MeV (Ref. 37) were measured earlier. The ^{238}Pa isotope was accumulated by bombarding uranium stacks in a neutron flux generated in a thick beryllium target bombarded by deuterons. The neutron energy spectrum fell in the range from 8 to 20 MeV. The average cross section of the reaction $^{238}\text{U}(n, p)$ was estimated from this spectrum, the excitation function of the (n, p) reaction, and the known cross section at neutron energy 14.7 MeV.

In other cases, the cross sections were determined from the intensity of the γ lines in the decay of ^{234}Pa and ^{238}Pa nuclei. A multiple-target assembly was used to increase the intensity of the radiation under study. The particle flux fell directly on 20 uranium or thorium targets of thickness $100 \mu\text{g}/\text{cm}^2$. Before the bombardment of the uranium, the targets were packed close together. After the end of the bombardment cycle the layers were moved 4 mm from each other, and polyethyleneterephthalate film serving as a practically background-free track detector was inserted periodically into the gaps. Fission-fragment detectors were introduced into the gaps between them after the bombardment. Successive replacement of the detectors at specified time intervals allowed measurement of the fragment time distribution and construction of the decay curve.

Despite the use of the multiple-target assembly, the number of recorded fragments remained insignificant. It was necessary to analyze carefully the possible sources of background and to take measures to eliminate them. By improving the technique in all the experiments except for bombardment by neutrons of energy 14.7 MeV, the observed number of fragments accompanying delayed nuclear fission was made to exceed the background.

The number of recorded fragments proved insufficient for determining the half-lives of the observed activities with satisfactory accuracy. However, the data obtained were consistent with the known half-lives of ^{238}Pa and ^{236}Pa . Analysis of the nuclear reactions occurring simultaneously with the studied ones led to the conclusion that none of the other possible products of these reactions could be the source of the fragment activity, owing both to the short lifetime of spontaneously fissioning shape isomers in this range of nuclei ($\sim 10^{-6}$ sec) and to the long half-lives with respect to spontaneous fission.

The numbers of recorded fission-fragment tracks in all the experiments were normalized to the yield of prompt-

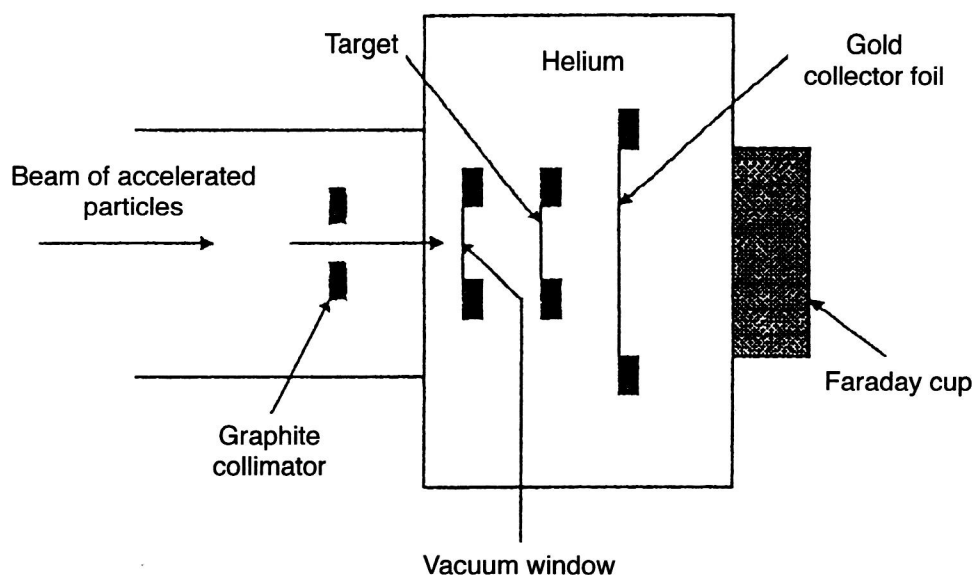


FIG. 16. Scheme of the ^{244}Es emitting block in the synthesis of $^{246\text{m}}\text{Es}$: $^{244}\text{Es}(t,p)^{246\text{m}}\text{Es}$.

fission fragments. The yield was determined from the γ emission of the ^{140}Ba fragment. The resulting data allowed the calculation of the cross section σ_{DF} for producing fragment activity and the delayed-fission probability $P_{\text{DF}} = \sigma_{\text{DF}}/\sigma$. Delayed fission of the ^{234}Pa nucleus was not observed.

Batist *et al.*³⁸ studied the delayed fission $^{236}\text{Pa} \rightarrow ^{236}\text{U} \rightarrow \text{ff}$ in the reaction $^{238}\text{U}(p,2pn)^{236}\text{Pa}$. A 1-GeV proton beam bombarded a uranyl nitrate target containing 5 g of uranium. The time for a single bombardment was 7 min. After a 6-min chemical separation of protactinium from the bombarded target matter, the protactinium fraction was placed between mica fission-fragment detectors. Simultaneously with the detection of fission fragments, the γ spectrum of the products of the fraction was measured by means of a germanium γ detector. The total number of synthesized ^{236}Pa nuclei was determined from the decrease of the intensity of the line with γ energy $E = 642$ keV characteristic of ^{236}Pa . As a result, the delayed-fission probability of ^{236}Pa was found to be about 10^{-9} in experiments using 1-GeV protons.

Hall *et al.*³⁹ studied the β -delayed fission $^{256\text{m}}\text{Es}(T_{1/2} = 7.6 \text{ h}) \rightarrow ^{256}\text{Fm}(T_{1/2} = 2.63 \text{ h}) \rightarrow \text{ff}$. The $^{256\text{m}}\text{Es}$ isotope was synthesized in the nuclear reaction $^{254}\text{Es}(t,p)^{256\text{m}}\text{Es}$. In the next stage, the einsteinium was separated from the other reaction products in an ion-exchange column. After the chemical separation, the decay in the transition of $^{256\text{m}}\text{Es}$ to ^{256}Fm was studied by measuring $\beta-\gamma$, $\gamma-\gamma$, and $\beta-f$ coincidences. It was possible to construct the level structure of the daughter nucleus ^{256}Fm and to record delayed-fission events.

The experiment was performed as follows. From the material containing ^{254}Es ($T_{1/2} = 276$ days), 0.1 μg of pure einsteinium was separated and electrolytically deposited on a beryllium backing of thickness 0.0125 mm covered with palladium. The einsteinium was precipitated on a disk of diameter 0.2 cm. The target thickness, measured by means of α spectroscopy, was 2.5 $\mu\text{g}/\text{cm}^2$. The target was cooled by a helium flow (see Fig. 16). Owing to the high activity of the einsteinium, all the cooling gas passed through filters, and

detectors were placed near the target chamber to monitor the air activity. The target was bombarded for about 7 hours by tritium ions accelerated to 16 MeV with an intensity of 6–10 μA . This tritium energy corresponded to the maximum yield of $^{256\text{m}}\text{Es}$. Here the cross section for $^{256\text{m}}\text{Es}$ production was $1.6 \times 10^{-26} \text{ cm}^2$. The recoil products were accumulated on a gold collector. After the bombardment, the target and the target chamber were allowed to cool off for an hour. During this time the short-lived nuclei, including ^{256}Es ($T_{1/2} = 25$ min), decayed. After the bombardment, the einsteinium was separated by ion-exchange methods from the other reaction products and the target material. Double cleaning was done to eliminate the spontaneously fissioning isotope ^{256}Fm . Then at the start of counting, fragments from the spontaneous fission of the daughter fermium did not complicate the measurements. Data on the level scheme of ^{256}Fm were obtained by recording $\beta-\gamma$ and $\gamma-\gamma$ coincidences, while fragments from the β -delayed fission of $^{256\text{m}}\text{Es}$ were recorded by using $\beta-f$ coincidences. The authors constructed a detailed level scheme for ^{256}Fm .

According to the data on $\beta-\gamma$ coincidences, the half-life of the isomer level at 1425 keV was $(70 \pm 5) \times 10^{-9}$ sec, which is significantly smaller than the value estimated on the basis of the systematics of K -forbidden transitions.

In the end, it was concluded that delayed fission activity of $^{256\text{m}}\text{Es}$ occurs after population of the level at 1425 keV.

Only two cases of delayed fission were observed. Fission from the isomer level at 1425 keV with spin and parity 7^- of the ^{256}Fm nucleus was apparently the first case, when the delayed fission was recorded as fission from the isomer state of the first well of the potential-energy surface. The very small fission branch (2×10^{-5}) of the level at 1425 keV confirms this conclusion. The partial half-life with respect to fission was estimated to be ~ 0.8 msec.

The experimental data on β -delayed fission in chains with parent nuclei of protactinium and einsteinium are given in Table III. Owing to the small cross sections for the formation of the parent nuclei of delayed-fission chains and the

TABLE II. Studied neutron-deficient delayed emitters.

Nucleus	$T_{1/2}$	P_{DF}	Nuclear reactions
^{180}Tl	$0.70^{+0.12}_{-0.09}$ sec	$\sim 10^{-6}$	
^{208}Ac	0.1 sec	-	$^{197}\text{Au}(^{20}\text{Ne}, 9n)^{208}\text{Ac}$
^{228}Np	60 ± 5 sec	-	$^{209}\text{Bi}(^{20}\text{Ne}, 3n)^{228}\text{Np}$
^{232}Am	1.4 ± 0.25 min	6.96×10^{-2}	$^{230}\text{Th}(^{10}\text{B}, 8n)^{232}\text{Am}$
	0.92 ± 0.12 min	$1.3^{+4}_{-0.8} \times 10^{-2}$	$^{237}\text{Np}(\alpha, 9n)^{232}\text{Am}$
	1.31 ± 0.04 min	$(6.9 \pm 1.0) \times 10^{-4}$	$^{237}\text{Np}(\alpha, 9n)^{232}\text{Am}$
^{234}Am	2.6 ± 0.2 min	6.95×10^{-5}	$^{230}\text{Th}(^{10}\text{B}, 6n)^{234}\text{Am}$
	2.6 ± 0.2 min	-	$^{233}\text{U}(^{11}\text{B}, \alpha 6n)^{234}\text{Am}$
	2.32 ± 0.08 min	$(6.6 \pm 1.8) \times 10^{-5}$	$^{237}\text{Np}(\alpha, 7n)^{234}\text{Am}$
^{238}Bk	144 ± 6 sec		
^{240}Bk	4 min	10^{-5}	$^{232}\text{Th}(^{14}\text{N}, 6n)$
^{242}Es	5–25 sec	$(1.4 \pm 0.8) \times 10^{-2}$	$^{205}\text{Tl}(^{40}\text{Ar}, 3n)$
^{244}Es	37 sec	10^{-4}	$^{236}\text{U}(^{14}\text{N}, 5n)$
			$^{237}\text{Np}(^{12}\text{C}, 5n)$
^{246}Es	8 min	3×10^{-5}	$^{238}\text{U}(^{14}\text{N}, 6n)$
^{248}Es	28 min	3×10^{-7}	$^{238}\text{U}(^{14}\text{N}, 4n)^{248}\text{Es}$
^{246}Md		6.5×10^{-2}	$^{209}\text{Bi}(^{40}\text{Ar}, 3n)$
^{248}Md	7 sec	6.5×10^{-2}	$^{239}\text{Pu}(^{14}\text{N}, 5n)$
^{250}Md	52 sec	2×10^{-4}	$^{243}\text{Am}(^{12}\text{C}, 5n)^{250}\text{Md}$

problems arising in the suppression of background due, for example, to uranium fission by delayed neutrons, γ emission from fragments, and the spontaneous fission of daughter nuclei, such experiments require a great deal of effort.

They are justified by the fact that they provide information about deep sub-barrier fission from an identified isomer level of the daughter nucleus.

Direct experiments to study neutron-rich nuclei, for which $Q_{\beta} \sim B_f$, i.e., nuclei which are quite far from the β -stability line, could in principle be carried out by using pulsed neutron fluxes from thermonuclear explosions. However, for obvious reasons the development of such techniques is extremely difficult. Moreover, underground thermonuclear devices are now prohibited in many countries. One can only hope that it will prove possible to obtain accelerated beams of radioactive heavy ions with large neutron excess in reactions in which neutron-rich parent isotopes in the region of delayed fission can be obtained.

At present, there are only indirect data on delayed fission of neutron-rich nuclei synthesized in pulsed neutron fluxes of underground thermonuclear explosions. The half-lives of the parent nuclei of the predecessors of delayed fission are too short for their delayed fission to be detected by the available slow techniques of separating isotopes of heavy elements.

2.11. Fission barriers of nuclei far from the β -stability line and delayed fission

Nuclear-fission barriers are the main characteristic determining the stability of the heaviest nuclei, including super-heavy elements. Most of the available experimental data on fission barriers pertains to nuclei lying in the β -stability valley in the region $90 < Z < 98$, $140 < N < 156$. The most detailed information about the characteristics of these nuclei has been obtained mainly in reactions of the type (d, pf) , (t, pf) , (t, df) , and (n, f) .

The current representation of the fission barriers of heavy nuclei and of their N and Z dependence rests on the concept of a strong influence exerted by shell effects on the nuclear-deformation energy, according to which nuclear shells are preserved in the deformation process, while only their characteristics are changed. The most fruitful approach to the theoretical study of fission barriers is the macro-microscopic method of calculating the nuclear-deformation energy, developed in Ref. 40 and, especially, in Refs. 41 and 42. The idea behind the method is that most of the total energy of the nucleus is calculated macroscopically, using the liquid-drop model or a generalization of it, while the contribution of internal-structure effects is included by the shell correction and the pairing correction. Thus,

$$E(q, N, Z) = \tilde{E}(q, N, Z) + \delta E(q, N, Z), \quad (13)$$

where q is the set of deformation parameters determining the shape of the nucleus, $E(q, N, Z)$ is the macroscopic part of the total energy describing smooth variations of E , and $\delta E(q, N, Z)$ is the microscopic correction reflecting the local fluctuations of the energy E and calculated by the Strutinsky method, where some single-particle potential is used for the deformed nuclear shapes. Study of the surface $E(q, N, Z)$ at the extrema leads to determination of the fission barriers.

There are several versions of the macro-microscopic approach which preserve the basic idea but use a variety of methods to parametrize the shape of the nuclear surface q , by choosing a specific model for calculating the smooth part E and a single-particle potential to calculate the microscopic corrections δE . The variants of the method lead to very similar results for nuclei lying in the β -stability valley. It is therefore difficult to prefer any particular version of the macro-microscopic approach on the basis of the experimental results from studying the properties of nuclei only in the β -stability valley. The situation is different far from the β -stability line. The predictions based on different variants

TABLE III. Experimental data on β -delayed fission.

β transition	Q , MeV	Reaction	E , MeV	σ , cm ²	σ_f , cm ²	P_{DF}
$^{238}\text{Pa} \rightarrow ^{238}\text{U}$	4.0	$^{238}\text{U}(n, p)$	14.7	1.5×10^{-27}	10^{-33}	6×10^{-7}
		(n, p)	8–20	3.0×10^{-27}	5×10^{-33}	1.0×10^{-8}
		$^{238}\text{U}(\gamma, np)$	27	1.0×10^{-27}	10^{-36}	10^{-9}
$^{236}\text{Pa} \rightarrow ^{236}\text{U}$	3.1	$^{238}\text{U}(d, \alpha)$	18	1.0×10^{-28}	3×10^{-38}	3×10^{-10}
		$(p, 2pn)$	1000			10^{-9}
$^{234}\text{Pa} \rightarrow ^{234}\text{U}$	2.2	$^{232}\text{Th}(\alpha, np)$	36	3.0×10^{-27}	10^{-38}	3×10^{-12}
^{256m}Es		(t, p)	16			Fission from the level at 1425 keV, 2×10^{-5}

TABLE IV. Experimental and calculated values of the fission barriers of isotopes of transuranium elements.

Nucleus	E_A exp., MeV	$E_A(S)$, MeV	p^{exp}
^{232}Pu	4.0–4.5	3.5–4.3	$1.3^{+4}_{-0.8} \times 10^{-2}$
^{244}Cf	5.3	5.1–5.6	5×10^{-4}
^{248}Fm	5.7	5.3–5.9	3×10^{-3}
^{248}Cf	>5.8	5.4–5.9	$<10^{-7}$
^{240}Cm	4.7	4.9–5.5	10^{-5}

of the model differ from each other not only quantitatively, but also qualitatively. For example, the Myers and Swiatecki variant of the liquid-drop model⁴⁰ and the droplet model give completely opposite behaviors of the macroscopic part of the barrier as a function of $(N-Z)/A$. This leads to large divergences for the barriers of nuclei far from the β -stability line, and makes it possible to judge the degree to which a given model is applicable for calculating the barriers. However, the barrier parameters of such nuclei cannot be measured at low excitation energies in induced-fission reactions⁴³ or in reactions producing spontaneously fissioning isomers, because there are no suitable targets or spontaneously fissioning isomers in this nuclear region.

The only possibility of determining the parameters of nuclei very far from the β -stability line is by studying delayed fission. The planning of experiments to study neutron-deficient nuclei 15–20 neutrons away from the β -stability line began back in 1981 (Ref. 31). At present, the values of the fission barriers of a number of neutron-deficient as well as neutron-rich nuclei are known from the data on their delayed fission. Among these are, in particular, the isotopes ^{232}Pu and ^{234}Pu .

The height of the fission barrier of ^{232}Pu calculated on the basis of data on the delayed fission of ^{232}Am , assuming $S_\beta = \text{const}$ (Ref. 19), does not agree with that calculated by the Strutinsky method. Izosimov and Naumov⁴⁵ calculated the fission-barrier heights for ^{232}Pu from measurements of delayed fission, using various models of nuclear fission for a two-hump barrier and various assumptions about the nature of the strength function of β decay, and showed that it is necessary to include the resonance structure of the strength function.

Later on, the same authors estimated^{44,45} the fission-barrier heights and probabilities P_{DF} of the nuclei ^{232}Pu , ^{244}Cf , ^{246}Fm , ^{248}Cf , and ^{240}Cm by using more realistic models and including the nonstatistical strength function of EC with Gaussian peaks centered at the 0^+ and 2^+ levels and of half-width 1 MeV. Calculation of the fission through a two-hump barrier, taking into account the partial mixing of states in the first and second wells, gave a delayed-fission probability coinciding with that obtained experimentally. This suggests that the barriers obtained by the Strutinsky method are consistent with the data on the delayed-fission probabilities (see Table IV).

In Ref. 46, Izosimov estimated the fission-barrier parameters of nuclei synthesized near the $Z=82$ shell. For these neutron-deficient nuclei the neutron binding energy is ≥ 11 MeV, and so there is no neutron emission in the decay

TABLE V. Results of calculating the probability of β -delayed fission P_{DF} for various barrier heights B_f of the ^{180}Hg nucleus.

B_f , MeV	$\hbar\omega$, MeV	Δ , MeV	P_{BDF} (GS)	Γ_{BW} , MeV	P_{BDF} (BW)
8	0.5	1	1.5×10^{-1}	-	-
9	0.5	-	-	1	1.5×10^{-2}
				2	3.1×10^{-2}
10	1.0	173 ± 5	1.4×10^{-5}	1	1.7×10^{-3}
			9.3×10^{-5}	2	3.7×10^{-3}
10	0.5	175 ± 5	5.8×10^{-7}	1	7×10^{-4}
			1.2×10^{-5}	2	1.5×10^{-3}
11	1.0	99.8 ± 2.0	3.2×10^{-8}	1	1.1×10^{-5}
			2.4×10^{-7}	2	2.3×10^{-5}
12	1.5	73.5 ± 1.4	9.5×10^{-4}	1	2×10^{-8}
			1.8×10^{-7}	2	4.1×10^{-8}
13	1.5	100.6 ± 2.0	-	1	2.9×10^{-8}
				2	6×10^{-8}
		74 ± 1.4			
		91 ± 0.1			
		134.8 ± 0.1			

Note: GS means that S_β is represented by a Gaussian with half-width Δ , and BW means that S_β is given as a Breit–Wigner distribution with width Γ_{BW} . The maximum of S_β occurs at $E=6.8$ MeV. The experimental estimate is $P_{\text{DF}} \approx 10^{-6}$ and $Q_\beta = 11$ MeV.

of these nuclei. The same is true of delayed protons held by the Coulomb barrier and not noticeably contributing to the total width of the main daughter-nucleus excitation channel competing with delayed fission, i.e., γ decay. The fission widths were calculated for various assumptions about the symmetry of the nuclear deformation at saddle points. It was assumed that a difference in the entrance channels is weakly reflected in the fission probabilities.

The results of calculating P_{BDF} are given in Table V. For the ^{180}Hg nucleus a 1-MeV change in the barrier height leads to a change of the delayed-fission probability by three orders of magnitude. Therefore, by comparing the calculated and measured values of P_{BDF} , the barrier height of as exotic a nucleus as ^{180}Hg can be determined with an accuracy of 1 MeV. With the parameter $\hbar\omega = 1$ MeV, the barrier height of ^{180}Hg is ~ 11 MeV. For the isotope ^{174}Pt , the probability of delayed fission is $\sim 10^{-6}$ and the barrier height is 10 MeV.

In general, a correct analysis of the experimental data is possible if the structure of the β -transition strength function is known. For some nuclides, for example, for ^{188}Pb and ^{190}Pb , it is difficult to estimate the value of B_f without experimentally measuring S_β . And still for many nuclei the uncertainties due to the calculated values of S_β , Γ_f , and Γ_γ limit the accuracy with which the barrier height can be determined to ~ 1 MeV.

Information on the fission barriers of nuclei ~ 20 nucleons away from the β -stability line, for example, ^{208}Ac and ^{180}Hg , therefore becomes accessible.

2.12. The effect of delayed fission on the synthesis of heavy elements in pulsed thermonuclear neutron fluxes

The duration of the neutron pulse from an underground thermonuclear explosion is of order 10^{-6} sec. During this time there is multiple neutron capture by the target nuclei. The total time for neutron capture is much smaller than the

β -decay half-lives of all the synthesized neutron-rich nuclei. Therefore, the nuclear-transformation process in such a pulsed flux occurs in two stages: synthesis of neutron-rich nuclei with various mass numbers A and atomic number Z equal to the target atomic number, and production of heavy β -stable elements and fission fragments as a result of spontaneous fission and delayed processes accompanying β transformations. Several experiments have been carried out for high neutron fluxes. In the Maik thermonuclear explosion, the flux was about 2.0×10^{24} neutrons/cm². Roughly the same value was attained in 1962 in the Anacostia experiment. In the Par and Barbel experiments in 1964 and the Cyclamen experiment in 1966 the flux reached 4.5×10^{24} and 1.2×10^{25} neutrons/cm², respectively.⁴⁷ A flux of 4.5×10^{25} neutrons/cm² was obtained in the HUTCH experiment in 1969.⁴⁸

Uranium and thorium targets have been bombarded in the neutron fluxes of thermonuclear explosions. The target in the Cyclamen experiment contained a certain amount of ²⁴³Am. When the pulsed neutron bombardment of the uranium target stopped, isotopes of uranium up to ^(238+m)U had been produced, where m , the maximum number of neutrons sequentially captured by the original target nuclei, lies in the range 17–19.

Two delayed processes play an important role in β -transformation chains: fission and delayed neutrons. Delayed fission transforms heavy nuclei into fragments, while neutron emission only reduces the mass by several units and preserves a heavy nuclide. The fission probability of the daughter nucleus ($Z+1, A$) after the β decay of the parent nucleus (Z, A) has a complicated dependence on the nuclear characteristics.

It should be noted that the decay energy Q_β in a decay chain of products of pulsed neutron fluxes reaches values at which the excitation energy of the daughter nucleus E^* is sufficient for the emission of several neutrons. However, such processes do not play an important role in real neutron fluxes in thermonuclear explosions. The values of Q_β determining the β -decay process are calculated by using various mass formulas suitable for specific nuclei with large neutron excess. A mass formula in which the mass of the deformed nucleus is a function of not only Z and A but also the deformation parameter determined by extrapolation of the existing data to the region of heavy neutron-rich nuclei is considered satisfactory for this problem. The effect of the $Z=114$ and $N=184$ neutron shells is also taken into account.

The fission barriers of nuclei which are the products of multiple neutron capture by a heavy target are calculated by the Strutinsky macro-microscopic method. The parameters of the barriers of even–even nuclei involved in the transformation chain are known.⁴⁹ The fission barriers of odd–odd and even–odd nuclei determine by interpolation the barrier heights of even–even nuclei (an increase of the barrier height by 0.70 MeV for even–odd nuclei and by 0.80–1 MeV for odd–odd nuclei).

If the β -decay energy is lower than the total energy Q_β , the strength function S_β determines the main decay characteristics. In the first approximation the strength function of a

neutron-rich nucleus is assumed to be proportional to the level density of the daughter nucleus.¹¹

On the basis of the Fermi-gas model, the level density of the daughter nucleus is written as

$$\rho(E) = C/U^2 \exp 2\sqrt{aU}, \quad (14)$$

where $a=0.125A$ and $U=E-\Delta$; $\Delta=0$, $12A^{-1/2}$, and $24A^{-1/2}$ for odd–odd, even–odd, and even–even nuclei, respectively.

In the region $A < 248$ all β -active nuclei have $Q_\beta < B_f$ if $Z \geq 92$, and so delayed processes have practically no effect on the yield and isotope content of elements synthesized in pulsed neutron fluxes. The situation changes when $A \geq 250$. In this region, for nuclei lying several neutrons away from the β -stability line, Q_β satisfies the condition $Q_\beta > B_f$, $Q_\beta > B_n$; as a result, the probabilities for delayed-neutron emission and delayed fission are fairly large, and the yield of nuclei with $A > 250$ depends on them.

The greatest losses to delayed fission occur on nuclei with even mass number A . This is due to the fact that this class includes odd–odd nuclei, the delayed-fission probability of which is manifested considerably earlier than for neighboring nuclei.

From the viewpoint of studying delayed processes, it is especially interesting to look at the general features of the mass distribution of products synthesized in the pulsed neutron flux of a thermonuclear explosion, the so-called inversion of the even–odd effect. The essence of this effect is the following. If the yield curves of nuclei with even and odd A are constructed, the first curve with even A initially lies above the curve with odd A . Then, as A increases, the yield curve for nuclides with odd A begins to move above the curve with even A —the effect is inverted.

Several assumptions have been made in order to explain this phenomenon, but all are unsuccessful (see, for example, Ref. 50).

If we take into account the effect of delayed fission on nucleosynthesis, the inversion of the even–odd effect and its distinctive features are naturally explained.

As already mentioned, if the mass number of a neutron-rich nucleus is $A < 250$, the excitation energy of the daughter nucleus is smaller than the fission-barrier height and the neutron binding energy B_n . Therefore, here delayed processes are either forbidden, or they occur with very small probability. The cross section for neutron capture by even isotopes of uranium is smaller than that for odd ones, and so the yield of even–even isotopes in the region $A < 250$ must be larger. This follows from the fact that for two neighboring nuclei in the chain of uranium isotopes capturing neutrons we have $N_1/N_2 \approx \sigma_2/\sigma_1$, where N_1 is the number of nuclei with capture cross section σ_1 , and N_2 is the number of nuclei with capture cross section σ_2 .

When delayed fission occurs with high probability, the losses in the transformation chains of heavy nuclei with even A are manifested much earlier than for nuclei with odd A , because it is nuclei with even A that contain odd–odd nuclei, for which the conditions for delayed fission to occur with high probability, $Q_\beta > B_f$, are satisfied at a smaller distance away from the β -stability line.

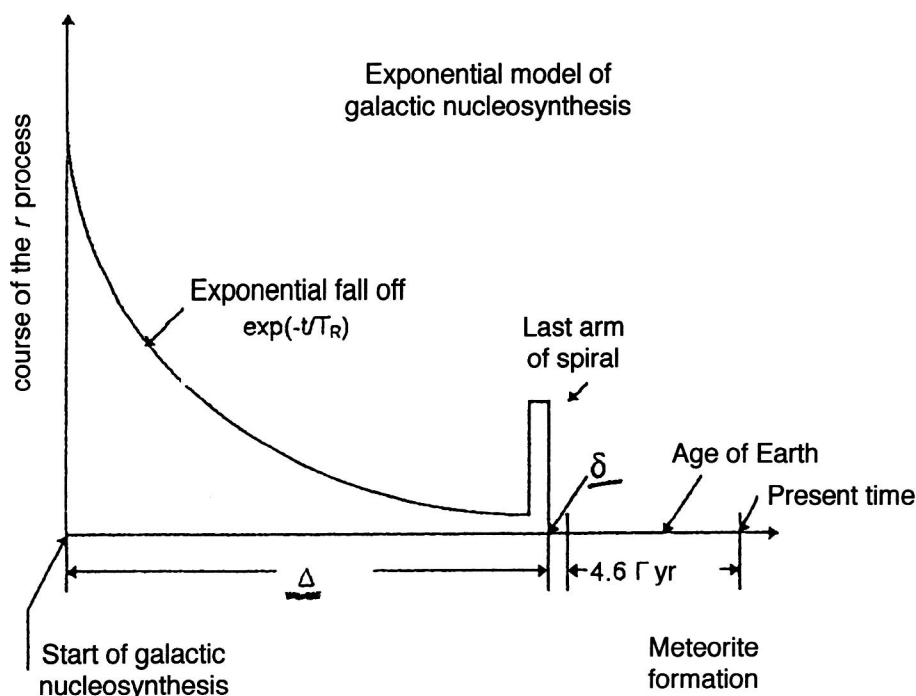


FIG. 17. Galactic nucleosynthesis. Time intervals.

Calculation of the isotope yield reveals a relation between the inversion effect and the initial ratio of concentrations of even and odd isotopes of uranium, and also the neutron flux nvt . In the HUTCH experiment, the odd–even inversion was observed starting at $A=255$, and in the Par experiment the effect was farther to the left at $A=252$. Therefore, as the flux varies from 7×10^{24} (Par) to 4.5×10^{25} (HUTCH), the inversion effect shifts toward larger A by three or four units.

If delayed fission is included in the analysis of the transformations of a chain of neutron-rich nuclei synthesized in a pulsed neutron flux from a thermonuclear explosion, the simple model not only predicts the appearance of the effect, but also qualitatively explains its shift as a function of the flux.

In order to obtain a quantitative picture of the isotope yield in the bombardment of various targets by pulsed neutron fluxes with bombardment time $T_0 \gg T_\beta$, where T_β is the shortest β -decay period in the transformation chain of heavy neutron-rich nuclei, it is necessary to develop more rigorous theoretical models.

2.13. Chronometric pairs and delayed fission

Astronomers have observed a tendency for extra-galactic nebulas to recede from our galaxy. The recession speed v (in km/sec) is proportional to the distance R to the galaxy: $v = HR$, where H is the Hubble constant, lying in the range 50–100 (km/sec)/Mpc, and the age of the universe T_u is estimated as $1/H$ (this expression is valid for $v \ll c$). If we take $H = 75$ (km/sec)/Mpc, then $T_u = 13 \times 10^9$ yr.

An alternative to the astronomical method of determining the age of the universe is the nuclear method. It amounts to calculating the time which has passed since the formation of the elements of the universe in the intense neutron fluxes of the r process, which is commonly assumed to occur at

neutron densities $\sim 10^{20} - 10^{30} \text{ cm}^{-3}$ and temperatures $\sim (0.5 - 5.0) \times 10^9$. The system of nuclear-transformation equations during the neutron bombardment and after its fall-off are written down. In the end, a relation is obtained between chronometric pairs— isotopes with half-lives comparable to the age of the universe: $^{232}\text{Th}/^{238}\text{U}$, $^{235}\text{U}/^{238}\text{U}$, and $^{244}\text{Pu}/^{238}\text{U}$, and the value of T_u .

The most extensive calculations of the duration of nuclear synthesis of the elements of the universe and the age of the galaxy were performed by Tielmann *et al.*,⁵¹ who used an exponential model of galactic nucleosynthesis.

Over the path of an r process, heavy elements are successively accumulated by neutron capture, become saturated, and undergo β decay. Delayed neutrons and nuclear fission form the final yield curve of the heavy elements in approaching the β -stability valley. By comparing the calculated ratios of chronometric pairs, in particular, the pair $^{232}\text{Th}/^{238}\text{U}$, with the values determined experimentally and rescaled to the time of formation of the solar system, it is possible in principle to obtain the duration of nucleosynthesis and the age of the galaxy.

In the opinion of the authors of Ref. 51, the predictions for the age of the galaxy on the basis of the element abundances are systematically too low. That study predicts a region of nuclei near $Z=94$ and $N=164$ with delayed-fission probability equal to 100%, which obstructs the route to the formation of superheavy elements.

Using the exponential model of galactic nucleosynthesis, the age of the galaxy was found to be⁵¹ $(20.8_{-4}^{+2}) \times 10^9$ yr, which is larger than the estimate based on the chronometric pair $^{187}\text{Re}/^{187}\text{Os}$. The age of the galaxy is made up of three quantities (see Fig. 17):

$$T_u(\Delta + \delta + 4.6) \times 10^9 \text{ yr.} \quad (15)$$

Here Δ is the time to produce elements in the neutron flux of

the r process, δ is the time to produce meteorites, and 4.6 is the age of the Earth. All quantities are expressed in gigayears.

However, in Refs. 52 and 53 it was shown that in the studies by Tielmann *et al.*⁵¹ the delayed-fission probabilities are too high, and the age of the universe does not exceed 15 Gyr. Nevertheless, calculations using various models of the strength functions and other parameters determining the course of nucleosynthesis confirm that there is always a region with very high probability for the delayed fission of heavy neutron-rich nuclei.

The authors of Refs. 54 and 55 conclude that delayed fission can decrease the yield of superheavy elements by a factor of 2.6 to 190 in the regions $Z=110$ – 112 and $A=291$ – 297 for the surface-symmetry constant of the liquid-drop model equal to 1.79 and 2.3.

If we review the methods for calculating element formation in fast neutron fluxes, we arrive at the conclusion that at present, even with the most modern approach for theoretically calculating the nuclear age of the universe, all the estimates which have been obtained are not really reliable, since the necessary information about the characteristics of heavy neutron-rich nuclei is still not available. According to the theoretical estimates, a high probability of delayed fission must be observed for nuclei with neutron excess greater than 10, compared with the presently known neutron-rich isotopes. Of course, experimental data on such nuclei would allow the age of the universe to be determined more accurately. However, there is still no way to synthesize such nuclei. At present, the most reliable value of the age of the universe is thought to lie in the range 13–15 Gyr.

3. CONCLUSION

The experimental and theoretical studies of delayed fission have passed through the following main stages.

- The synthesis of three neutron-deficient nuclei with half-lives on the order of a minute (^{228}Np , ^{232}Am , and ^{234}Am) in accelerated heavy-ion beams, measurements of their lifetimes, and the prediction that their decay mechanism is delayed fission (1967). Later on, the delayed emitters ^{232}Am and ^{234}Am in the minute range became the testing ground for detailed study of delayed fission. Their long lifetimes made it possible to use not only nuclear-physics methods, but also chemical methods of study.

- Detailed interpretation of the decay of the nuclear predecessors ^{232}Am and ^{234}Am entering into the delayed-fission process (1972).

- The discovery of a significant asymmetry of the fission fragments of the isotopes ^{234}Am and ^{232}Am in the symmetric distribution of the total kinetic energy TKE containing only a single component, and in the fission of the daughter nuclei ^{234}Pu and ^{232}Pu , characterized by average values of the TKE equal to 173 ± 5 MeV and 174 ± 5 MeV.

- The synthesis of delayed emitters of neutron-deficient isotopes with $Z > 95$ in beams of heavy ions ranging from berkelium to mendelevium.

- The study of β -delayed fission of neutron-rich nuclei obtained in nuclear reactions at accelerators.

- The discovery of a region of delayed fission of ultra-neutron-deficient nuclei to the left of the $N=126$ nuclear shell and then in the region $Z=82$, located 19–20 neutrons away from the β -stability line. This strongly confirmed the prediction about the nature of the decay of the nuclei $^{232,234}\text{Am}$ and ^{228}Np with half-life in the minute range.

- Study of the delayed fission of neutron-deficient nuclei with $Z > 95$.

- Study of the delayed fission of neutron-rich nuclei.

- Experimental measurement of the main characteristics of delayed fission—the delayed-fission probabilities P_{DF} and the production cross sections σ_{EC} and σ_{DF} for nuclei undergoing electron capture and delayed fission.

- Direct proof that there exists a new type of radioactive decay, delayed fission, by recording coincidences of x rays from plutonium with fission fragments of the daughter products of the nuclei ^{232}Am and ^{234}Am , namely, ^{232}Pu and ^{234}Pu , and also by recording coincidences of fission fragments of the daughter product $^{246\text{m}}\text{Es}$ of the isotope ^{246}Fm with β particles.

- Study of the energy and mass distributions of fragments from the delayed fission of ^{232}Pu and ^{234}Pu . The symmetric distribution of the total kinetic energy is characterized by the average values 173 ± 5 MeV and 174 ± 5 MeV.

Thus, the full set of experiments showed that delayed fission is a common decay channel of heavy nuclei with sufficiently large Q_{β} .

These results were used in theoretical studies to determine the fission-barrier heights of nuclei fairly far from the β -stability line. They were used as the basis for a new approach to calculating the strength functions.

The discovery of delayed fission stimulated the development of studies of nuclear cosmochronology and allowed the understanding of some processes occurring in thermonuclear explosions.

Currently, the main problem in this area is the experimental and theoretical study of neutron-rich nuclei. With the development of techniques for accelerating radioactive nuclei it may become possible to move to a region of such nuclei much farther from the β -stability line than at present.

The knowledge about the delayed fission after EC $^{228}\text{Np} \rightarrow ^{228}\text{U} \rightarrow \text{ff}$ is still completely insufficient, even though the half-life on the order of a minute allows detailed studies, and the structure of ^{238}U is of particular interest. The possibility of learning about the level structure in the second potential well of shape isomers in the process of delayed fission is also worthy of attention.

¹V. I. Kuznetsov, N. K. Skobelev, and G. N. Flerov, *Yad. Fiz.* 4, 99 (1966) [*Sov. J. Nucl. Phys.* 4, 70 (1967)].

²V. I. Kuznetsov and N. K. Skobelev, *Yad. Fiz.* 5, 1136 (1967) [*Sov. J. Nucl. Phys.* 5, 810 (1967)].

³V. I. Kuznetsov, N. K. Skobelev, and G. N. Flerov, *Yad. Fiz.* 5, 271 (1967) [*Sov. J. Nucl. Phys.* 5, 191 (1967)].

⁴V. I. Kuznetsov, N. K. Skobelev, and G. N. Flerov, *Yad. Fiz.* 4, 279 (1966) [*Sov. J. Nucl. Phys.* 4, 202 (1967)].

⁵V. I. Kuznetsov, N. K. Skobelev, and G. N. Flerov, *State Register of Discoveries, Otkrytie* No. 160, with priority from 12 July 1971.

⁶Yu. P. Gangrskii, M. B. Miller, L. V. Mikhaïlov, and I. F. Kharisov, *Yad. Fiz.* 31, 306 (1980) [*Sov. J. Nucl. Phys.* 31, 162 (1980)].

⁷H. I. Hall *et al.*, *Phys. Rev. C* 42, 1480 (1990).

- ⁸H. V. Klapdor, C.-O. Wene, I. N. Izosimov, and Yu. W. Naumov, *Z. Phys. A* **292**, 249 (1979).
- ⁹D. L. Hill and J. A. Wheeler, *Phys. Rev.* **89**, 1102 (1953).
- ¹⁰K. L. Kratz and G. Herrmann, *Z. Phys.* **263**, 435 (1973).
- ¹¹I. N. Izosimov and Yu. V. Naumov, *Izv. Akad. Nauk SSSR, Ser. Fiz.* **42**, 2248 (1978) [*Bull. Acad. Sci. USSR, Phys. Ser.*].
- ¹²Yu. V. Naumov, A. A. Bykov, and I. N. Izosimov, *Fiz. Élem. Chastits At. Yadra* **14**, 420 (1983) [*Sov. J. Part. Nucl.* **14**, 175 (1983)].
- ¹³A. Gilbert and A. G. W. Cameron, *Can. J. Phys.* **43**, 1446 (1965).
- ¹⁴N. K. Skobelev, *Yad. Fiz.* **15**, 444 (1972) [*Sov. J. Nucl. Phys.* **15**, 249 (1972)].
- ¹⁵V. I. Kuznetsov, Yu. A. Lazarev, Yu. Ts. Oganessian, and A. A. Pleve, in *Proceedings of the Intern. Conf. on Selected Aspects of Heavy Ion Reactions*, Saclay, 1982.
- ¹⁶Yu. Ts. Oganessian, V. I. Kuznetsov, and Yu. A. Lazarev, in *Proceedings of the Intern. Symp. on the Synthesis and Properties of New Elements* [in Russian], Dubna, D-780-556 (1980), p. 52.
- ¹⁷Yu. Ts. Oganessian, V. I. Kuznetsov, Yu. A. Lazarev, and A. A. Pleve, in *Proceedings of the Meeting on Experiments at the U-400 and the Physics Program of the Primary Experiments* [in Russian], Dresden, 1982, Book of Abstracts, D-7-82-891, (JINR, Dubna 1982), p. 50.
- ¹⁸L. P. Sommerville, M. I. Nurmia, A. Ghiorso, and G. T. Seaborg, *Annual Report, Lawrence Berkeley Laboratory* (1975), p. 39.
- ¹⁹D. Habs *et al.*, *Z. Phys. A* **285**, 53 (1968).
- ²⁰H. I. Hall *et al.*, *Phys. Rev. C* **41**, 618 (1990).
- ²¹R. D. Macfarlane and W. C. McHarris, in *Nuclear Spectroscopy and Reactions*, Part A, edited by J. Cerny (Academic Press, New York, 1974), p. 243.
- ²²Yu. P. Gangrskii, G. M. Marinescu, M. B. Miller, and I. F. Kharisov, *Yad. Fiz.* **27**, 894 (1978) [*Sov. J. Nucl. Phys.* **27**, 475 (1978)].
- ²³H. I. Hall *et al.*, *Phys. Rev. Lett.* **63**, 2548 (1989).
- ²⁴D. C. Hoffmann and M. M. Hoffmann, *Annu. Rev. Nucl. Sci.* **24**, 151 (1974).
- ²⁵J. H. Scofield, *At. Data Nucl. Data Tables* **14**, 121 (1974).
- ²⁶D. N. Poenaru, M. S. Ivascu, and D. Mazilu, in *Charged Particle Emission from Nuclei*, edited by D. N. Poenaru and M. S. Ivascu (CRC Press, Boca Raton, 1989), Vol. III, p. 41.
- ²⁷A. Viola, *Nucl. Data, Sect. B* **1**, 391 (1966).
- ²⁸J. P. Unik *et al.*, in *Proceedings of the Third IAEA Symp. on the Physics and Chemistry of Fission*, 1973 (IAEA, Vienna, 1974), Vol. 2, p. 19.
- ²⁹R. Hingmann *et al.*, Report GSI 85-1, GSI, Darmstadt (1985), p. 88.
- ³⁰Ch. Stodel *et al.*, in *Proceedings of the Intern. School-Seminar on Heavy Ion Physics*, Dubna, 1997, edited by Yu. Oganessian (World Scientific, Singapore, 1998), p. 712.
- ³¹V. I. Kuznetsov, *Fiz. Élem. Chastits At. Yadra* **12**, 1285 (1981) [*Sov. J. Part. Nucl.* **12**, 511 (1981)].
- ³²Yu. Ts. Oganessian and Yu. A. Lazarev, in *Treatise on Heavy Ion Science*, edited by D. A. Bromley (Plenum Press, New York, 1985).
- ³³Yu. A. Lazarev *et al.*, *Europhys. Lett.* **4**, 893 (1987).
- ³⁴É. E. Berlovich and Yu. N. Novikov, *Dokl. Akad. Nauk SSSR* **185**, 1025 (1969) [*Sov. Phys. Dokl.* **14**, 349 (1969)].
- ³⁵Yu. P. Gangrskii *et al.*, *Yad. Fiz.* **27**, 894 (1978) [*Sov. J. Nucl. Phys.* **27**, 475 (1978)].
- ³⁶G. Wolzak and H. Marinaga, *Radiochim. Acta* **1**, 23 (1963).
- ³⁷N. Trautman, R. Denig, and G. Herrmann, *Radiochim. Acta* **11**, 168 (1969).
- ³⁸L. Kh. Batist *et al.*, Preprint, Leningrad Nuclear Physics Institute, Leningrad (1977), p. 363 [in Russian].
- ³⁹H. L. Hall *et al.*, *Phys. Rev. C* **39**, 1866 (1989).
- ⁴⁰W. D. Myers and W. J. Swiatecki, *Nucl. Phys.* **81**, 1 (1966).
- ⁴¹V. M. Strutinskiĭ, *Yad. Fiz.* **3**, 614 (1966) [*Sov. J. Nucl. Phys.* **3**, 449 (1966)].
- ⁴²M. Brack *et al.*, *Rev. Mod. Phys.* **44**, 320 (1972).
- ⁴³B. B. Back *et al.*, *Phys. Rev. C* **9**, 24 (1974).
- ⁴⁴H. V. Klapdor *et al.*, in *Physics and Chemistry of Fission*, Vol. 1, p. 103.
- ⁴⁵I. N. Izosimov and Yu. V. Naumov, in *Proceedings of the Thirty-First Meeting on Nuclear Spectroscopy and Nuclear Structure* [in Russian], Samarkand (Nauka, Leningrad).
- ⁴⁶I. N. Izosimov, *Izv. Akad. Nauk SSSR, Ser. Fiz.* **57**, 29 (1993) [*Bull. Acad. Sci. USSR, Phys. Ser.*].
- ⁴⁷J. S. Ingley, *Nucl. Phys.* [sic].
- ⁴⁸G. A. Cowan, in *R. A. Welch Foundation Conferences on Chemical Research*, No. XIII, Houston, Texas (1969), p. 130.
- ⁴⁹I. G. Bell, in *Proceedings of the Intern. Conf. on the Study of Nuclear Structure with Neutrons*, Antwerpen, 1965, p. 127.
- ⁵⁰D. W. Dorn and R. W. Hoff, *Phys. Rev. Lett.* **14**, 440 (1965).
- ⁵¹F. K. Tielmann, J. Metzinger, and H. V. Klapdor, *Z. Phys. A* **309**, 301 (1983).
- ⁵²R. W. Hoff, in *Weak and Electromagnetic Interactions in Nuclei*, edited by H. V. Klapdor (Springer-Verlag, Heidelberg, 1986), p. 12.
- ⁵³R. W. Hoff, *Inst. Phys. Conf. Ser.* **14**, 343 (1988).
- ⁵⁴K. Aleklet, G. Nyman, and G. Rudström, *Nucl. Phys. A* **245**, 425 (1975).
- ⁵⁵P. Möller and J. R. Nix, in *Proceedings of the Third IAE Symp. on the Physics and Chemistry of Fission*.

Translated by Patricia A. Millard